

# Control of Pseudo-Sinusoidal Switched Reluctance Motor with Zero Torque Ripple and Damped Input Current Ripple

Le Du

Thesis submitted to the Faculty of the  
Virginia Polytechnic Institute and State University  
in partial fulfillment of the requirements for the degree of

Master of Science  
in  
Electrical Engineering

Jih-Sheng Lai, Chair  
William T. Baumann  
Wensong Yu

June 6, 2013  
Blacksburg, Virginia

Keywords: Switched Reluctance Motor, Torque Ripple, Power Ripple, Current Profiling,  
Pulsating Input Current, Control Scheme

Copyright 2013, Le Du

# Control of Pseudo-Sinusoidal Switched Reluctance Motor with Zero Torque Ripple and Damped DC Input Current Eliminations

Le Du

(ABSTRACT)

Switched reluctance motor(SRM)drives are favored in many industrial applications because of their cost advantage and ruggedness. However, the torque ripple and bus current ripple of SRM restrict its application range compared with traditional AC and DC motors due to the doubly salient pole structure and the highly non-linear coupling between torque, rotor position and phase current. As a result of the torque ripple on the shaft, unwilling large acoustic noises are generated. The large current ripple at the DC bus input requires large electrolytic capacitors for attenuation. However, electrolytic capacitors are of low reliability, which will reduce the duration of the control system. Because of these disadvantages, the acceptance of SRM by the industry, especially in servo-type applications which require stationary torque at low speed, is quite slow. In order to obtain high quality control, there have been many efforts in developing techniques for torque ripple attenuation. Primarily, two approaches are used to give a smooth torque. One is to improve the magnetic design, the other is to use sophisticated control techniques. Some torque control techniques have been proved to obtain a relatively good performance by simulations and experimental results. This thesis gives an alternative torque ripple minimization technique. Simulations and Experiments are conducted to show the effectiveness of this new control scheme. Under this new control scheme, the current controller are much easier to be designed under high speed application, which could be an advantage of it.

First, the SRM operating principle is presented. The torque of SRM is produced by the tendency of its moveable part shifting to a position where the inductance of the exited

winding is maximized. The torque ripple origin is discussed in terms of both magnetization and control. The torque ripple is produced during phase commutation interval because the phase current cannot rise from zero to the nominal value instantaneously due to the existence of the phase inductance.

Second, a new torque control scheme is proposed. The new torque control of SRM is split into two cascade sub-tasks. At first, a current reference for ripple free torque is determined. Then a current controller is designed to regulate the current in the stator winding to reference value. Simulations are conducted to verify the effectiveness of this torque control scheme in both ideal 'sinusoidal' SRM and a 'Pseudo-Sinusoidal' SRM.

Finally, a motor drive control system is built to implement the new control scheme. The motor is tested under different speeds to see the torque ripple produced in different speed ranges.

As a conclusion, the new control algorithm for constant torque and damped input bus current ripple is investigated. The advantages of this new torque control method are listed in the paper. Simulation and experimental results show the effectiveness of this new control method.

## Acknowledgements

For their support and direction over years, I would like to express my heartfelt gratitude to all my professors at Virginia Tech, without whom my research and this thesis would not have been possible. In particular, I am very grateful to my academic and research advisor Dr. Jason Lai. Without his generous and constant support, I could not finish my study program. His rigorous attitude toward research, valuable expertise, and extensive vision will guide me through my engineering profession for the rest of my life. My family and I are greatly indebted to him.

I next want to thank Dr. William T. Baumann and Dr. Wensong Yu for serving on my committee and giving me valuable suggestions on my thesis.

My gratitude extends to my Future Energy Electronics Center(FEEC) colleagues. It has been a great pleasure to work with the talented, creative, helpful and dedicated colleagues. I would like to thank all the members of our team: Dr. Deshang Sha, Mr. Gary Kerr, Mr. Bin Gu, Mr. Cong Zheng, Mr. Baifeng Chen, Mr. Rui Chen, Mr. Bo Zhou, Mr. Lanhua Zhang, Dr. Younghoon Cho, Mr. Seungryul Moon, Mr. Jason Dominic, Mr. Thomas LaBella, Mr. Ahmed Koran, Mr. Zakariya Dalala, Mr. Ben York, Mr. Zaka Ullah Zahid, Ms. Rachael Born, Mr. Eric Faraci, Mr. Tom Mao, Mr. Weihan Lai, Mr. Jiayi Zhang for their valuable assistants.

My deepest gratitude belongs to my parents, Dr. Shangfeng Du and Ms. Jie Ma. Their endless love, encouragement, and economic support helped me pass the hardest time in Virginia Tech and gave me the hope that I can finish the study in Virginia Tech when I almost wanted to give up. I would always remember those sleepless nights that you spent with me on skype keeping your eyes on me when I was desperate. Thank you, dad, for that you discussed daily with me on the research project, pushed me to finish the tasks on time

and gave me a lot of constructive suggestions. My mom, you gave me the power to persist on my study and the spiritual support to my life. Thank you for your support over these years.

# Contents

<b>1</b>	<b>Introduction</b>	<b>1</b>
1.1	Research Background . . . . .	1
1.2	Literature Review on SRM Torque Ripple Minimization . . . . .	3
1.2.1	Torque Sharing Function(TSF)Technique . . . . .	3
1.2.2	Nonlinear Control . . . . .	6
1.2.3	Intelligent Control . . . . .	8
1.3	Challenges to SRM Torque Ripple Minimization . . . . .	13
1.4	‘Pseudo-sinusoidal’ SRM . . . . .	14
1.5	Thesis Outline . . . . .	14
<b>2</b>	<b>Operating Principle and Mathematical Model</b>	<b>17</b>
2.1	Operating principle . . . . .	17
2.2	Switched Reluctance Machine Mathematical Model . . . . .	19
2.2.1	Equivalent Circuit . . . . .	19

2.2.2	Torque Equation . . . . .	20
2.2.3	Instantaneous Torque Generation . . . . .	20
2.2.4	Indealized Induction Model . . . . .	24
2.3	Control strategy . . . . .	26
2.3.1	Single Pulse Operation . . . . .	26
2.3.2	Voltage Chopping Control . . . . .	28
2.3.3	Current chopping control . . . . .	28
2.4	Variable speed Control for Switched Reluctance Motor Drive . . . . .	29
2.4.1	Summary . . . . .	30
<b>3</b>	<b>Torque Ripple Minimization in SRM</b>	<b>32</b>
3.1	Origin of Torque Ripple in SRM . . . . .	32
3.2	New Torque Minimization Control Scheme . . . . .	35
3.3	Implementation for Pseudo-sinusoidal SRM . . . . .	43
3.4	Summary . . . . .	45
<b>4</b>	<b>Implementation of New Torque Ripple Minimization Algorithm</b>	<b>47</b>
4.1	Hardware Implementation . . . . .	48
4.1.1	Pseudo-Sinusoidal Switched Reluctance Motor . . . . .	49
4.1.2	Power Stage . . . . .	49
4.1.3	Current Sensor . . . . .	50

4.1.4	Position Acquisition . . . . .	52
4.1.5	DSP Board . . . . .	52
4.1.6	Load Motor . . . . .	57
4.2	Software Layout . . . . .	57
4.3	Experimental Result . . . . .	60
4.4	Summary . . . . .	62
<b>5</b>	<b>Conclusions</b>	<b>63</b>
5.1	Conclusion and Future Work . . . . .	63
5.1.1	Summary . . . . .	63
5.1.2	Future Works . . . . .	64
5.2	Publications . . . . .	65



# List of Figures

1.1	Reluctance Motor Cross-Section . . . . .	2
1.2	SR variable speed system based on TSF . . . . .	4
1.3	Feedback Linearizing Control of SRM . . . . .	6
1.4	Neural Network Controller for SRM Drive . . . . .	9
1.5	The adaptive fuzzy controller for torque control of SRM . . . . .	11
1.6	Block diagram for ILC-based current controller . . . . .	12
2.1	Structure of SRM . . . . .	18
2.2	Equivalent Circuit for SRM . . . . .	20
2.3	Torque Generation . . . . .	21
2.4	Flux VS MMF . . . . .	22
2.5	Linearized Magnetic Characteristics for SRM . . . . .	24
2.6	Phase Inductance VS Rotor Position . . . . .	25
2.7	On-Angle for Single Pulse Operation . . . . .	27
2.8	Off-Angle for Single Pulse Operation . . . . .	27

2.9	Current Chopping . . . . .	29
2.10	Variable Speed Control System . . . . .	30
3.1	Torque Ripple Generation . . . . .	33
3.2	Inductance Profile . . . . .	36
3.3	MATLAB Simulation Schematic . . . . .	38
3.4	PSIM Simulation Schematic . . . . .	38
3.5	Simulation of the New Current Control Scheme . . . . .	39
3.6	Inductance Profile for Pseudo-sinusoidal SRM . . . . .	44
3.7	Current Profile for Pseudo-sinusoidal SRM . . . . .	44
3.8	Simulation Result for Pseudo-sinusoidal SRM . . . . .	45
4.1	SRM Drive with Torque Control . . . . .	48
4.2	Power Stage . . . . .	50
4.3	current transducer . . . . .	51
4.4	Encoder . . . . .	52
4.5	DSP Structure System . . . . .	53
4.6	AD7865 Inner Structure . . . . .	55
4.7	DSP Board . . . . .	57
4.8	Load Motor . . . . .	58
4.9	Experimental Setup . . . . .	59

4.10 Program Flow Chart . . . . .	59
4.11 Experimental Result at 500rpm . . . . .	60
4.12 Experimental Result at 1000rpm . . . . .	61

# Chapter 1

## Introduction

### 1.1 Research Background

The switched reluctance motor (SRM) is an electric motor in which the torque is produced by the tendency of its moveable part shifting to a position where the inductance of the excited winding is maximized [1]. The motor cross-section is illustrated in Figure 1.1. Both the stator and rotor have salient poles, therefore the motor is also referred as a doubly salient machine. The stator winding consists of a set of coils, each of which is wound on one pole. The rotor doesn't have coils or magnets. In motoring mode, the phases are excited when the respective phase inductance is increasing. For generating mode, the phases are excited when the inductance is decreasing.

Compared with permanent magnetic machines and induction machines, the SRM has a lot of advantages due to its low cost and simple rugged construction. Firstly, the doubly salient machine has the simplest structure among other types of machines. Windings are on the stators, but no windings or magnets on the rotor. Thereby, SRM finds applications in harsh

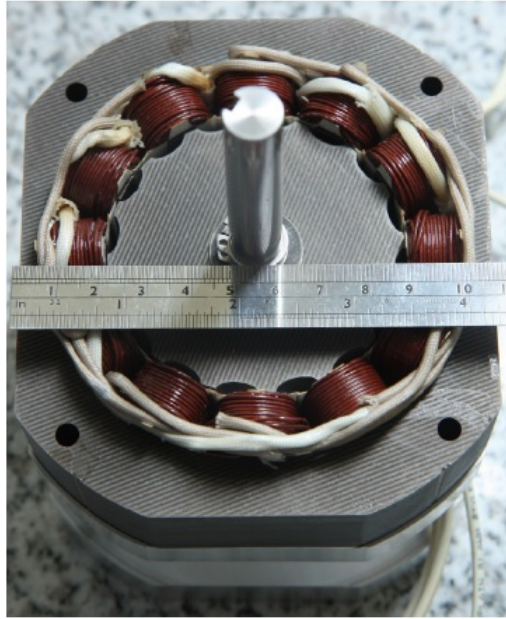


Figure 1.1: Reluctance Motor Cross-Section

environment with high temperature and vibration. Secondly, the stator current doesn't need to be bidirectional which greatly simplifies the design of power and control circuit. From control point of view, each phase can work independently. In other words, the SRM is able to operate with some phases disabled, which is an appealing characteristic for aviation and electrical vehicle applications. Besides, high starting torque and low starting current are attractive features for frequent startup applications.

However, SRM is inherently a highly non-linear system. Magnetic saturation together with salient stator and rotor poles give rise to a highly non-linear  $T - i - \theta$  characteristic which complicates the analysis and increases the difficulty to control. The ultimate outcome of all these nonlinearities is that high torque ripples are generated when the SRM is operated under conventional rectangular pulse excitation scheme. The torque ripple will introduce acoustic noise and bring in mechanical vibrations. Large electrolytic capacitors are used to attenuate the input bus current ripple. Therefore, in order to obtain high quality motor

drive performance, torque ripple minimization is indispensable.

## **1.2 Literature Review on SRM Torque Ripple Minimization**

As is mentioned before, the torque ripple minimization can be accomplished in two ways. One is magnetic design and the other is electric control. There are a large amount of research on torque ripple minimization in aspect of control, many of which will fall into one of the following techniques.

### **1.2.1 Torque Sharing Function(TSF)Technique**

A convenient electronic approach for minimizing torque ripple is to coordinate the torque production of the individual phases so that the total torque tracks the reference value generated by the position or speed control loop [2]. Instead of exciting one phase, two phases are conducted with controlled current contributing to a constant torque. The commutation angle is extended in torque sharing control scheme, as a result of which, the rise and fall rates of current in commutation intervals are smaller, leading to a easier current track. The control scheme for a SRM variable speed system based on torque sharing function is shown in Figure 1.2.

From the block diagram, it can be seen that the torque sharing function distributes different torque references in adjacent phases. With distributed torque reference, individual phase current command is given. As long as the phase current is able to track the reference, the torque ripple should be eliminated.

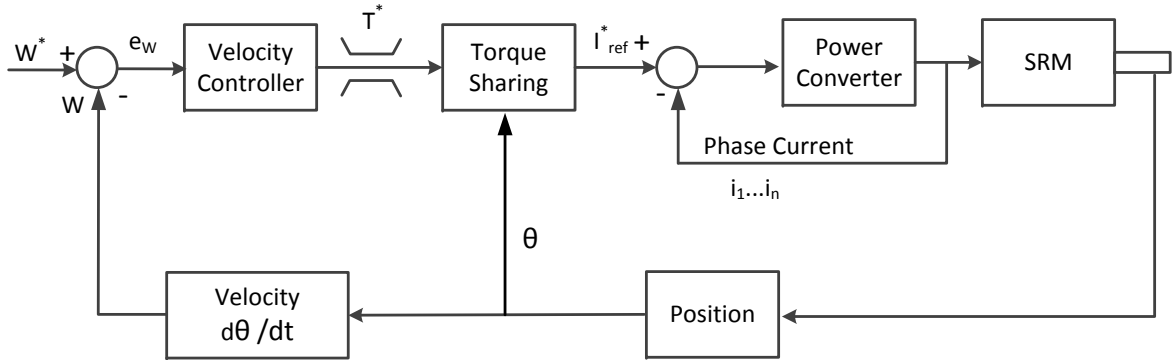


Figure 1.2: SR variable speed system based on TSF

The choice of TSF is not unique, and many functions satisfy the requirement of the torque ripple minimization control[3]. Several TSFs are proposed, some of which are with additional control objectives such as minimizing the power loss, the required voltage, etc. Ilic-Spong *et al.*[4] proposed an exponential torque sharing function with linear-feedback controller design to obtain good performance. However, only linearized magnetic model is considered, ignoring the saturation effect. If saturation is considered, large memory spaces are needed to store an accurate mathematical model.

Schramm *et al.*[5] proposes a trapezoidal torque sharing function. Meanwhile the commutation angle is selected based on current-position curves for difference torque levels curves to minimize the average and peak current. However, the current reference is derived off-line with bicubic spline interpolation computational algorithm, thereby, a large amount of memory is used to store the current data. Because of the off-line computation, the current reference is not adaptive to inaccuracy of the model, hence, the robustness is lost. From the outcome given by the paper, the current reference still have steep rise and fall with small commutation interval, around  $15^\circ$ . Therefore, a high bandwidth current control should be designed, but large torque ripple still exists when the motor is operating at high speed.

Another torque sharing function with sinusoidal profile was proposed by Husain *et al.*[6]. A

fixed-frequency varying-duty-cycle PWM current regulator is designed to control the phase current. In this control scheme, the commutation angle reaches about  $30^\circ$ . Simulation and experimental results show good performance at low speed.

Cubic TSF is used in [7],[8],[9] to develop a smooth function. The torques produced by two phases during phase commutation change with the rotor position according to a cubic polynomial[3].

Note that all the above torque sharing function is proposed based on the assumption that mutual inductance is ignored, therefore the model has some inaccuracies, an absolute flat torque cannot be obtained.

Kjare *et al.* in [10], the expected torque reference is given by both the SRM input voltage and the SRM rotor speed. The expected torque is converted to current reference with hysteresis current controller. This method considered other phase torque, improve the system robustness. However, the zero input voltage time interval is the function of the rotor speed.

Kim *et al.* in [11] points out the torque sharing functions are not unique and can be realized as long as several constraints are satisfied. Meanwhile, additional control objectives, such as reducing power loss, are considered in this paper. However, several implementation issues need to be considered to further optimize the torque sharing function.

The torque sharing functions proposed in the previous works defined the torque sharing functions only at a positive torque production region. This definition leads to a good performance at low-speed operation. As the speed increases, tail current occurs due to the limited bandwidth of the current controller. Torque ripple will increase at high-speed operation. [12],[13] extends the torque sharing function to the negative torque production region to guarantee enough time to decrease the current. The current reference is further smoother than that in previous works which has a promising application in high speed switched reluctance motor.



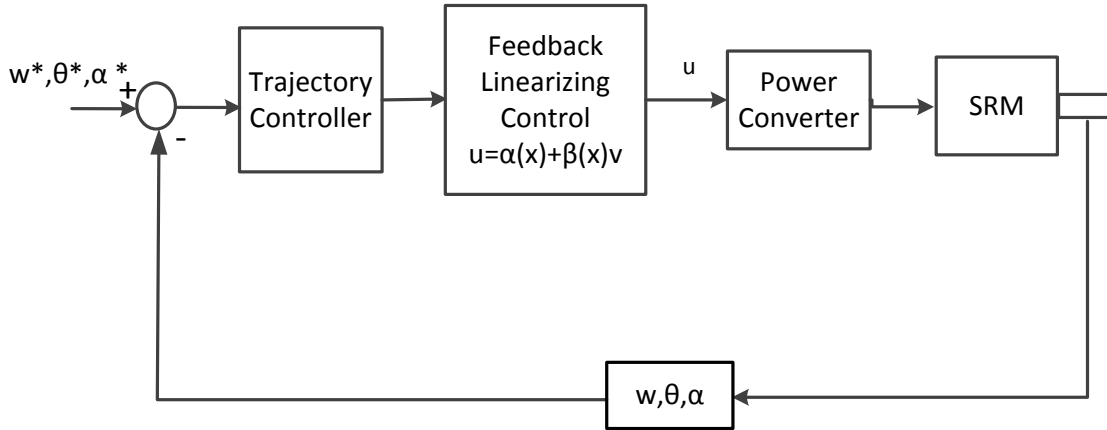


Figure 1.3: Feedback Linearizing Control of SRM

## 1.2.2 Nonlinear Control

### Feedback Linearization

Due to the highly nonlinear characteristic of the system, feedback linearizing control algorithms are designed to compensate the nonlinearities and decouple the link motions. In [14],[15], Ilic-Spong *et al.* firstly apply feedback linearizing control to the SRM variable speed system. The nonlinear state feedback control law is obtained and the system is transformed to a linear system by some transformation. The effect of stator phase current in the torque production is decoupled. The block diagram of the proposed feedback linearized SRM control system is shown in Fig 1.3.

However, the linear feedback controller depends on an accurate SRM model, lack of the robustness to the parameters uncertainty. In some cases, instability could happen if the linear feedback controller is not properly designed. In [16], S.K. Panda and S.K. Dash proposed a feedback linearizing controller based on Lyapunov's second method, which takes care of model uncertainty. The effectiveness is verified by the simulation.

The previous approach has the advantage of requiring large peaks in the phase current waveforms at low speeds. In [17], Wallace *et al.* developed a balanced commutator for SRM to limit the peaks and the rates of change of the reference currents. Therefore, the SRM can operate at a relatively large speed range. In [18],[19], the torque ripple reduction is quantified by simulation based on the approach proposed in [17].

Han-Kyung Bae and Krishnan in [20] consider the mutual inductance when two adjacent phases are excited. A torque sharing function is proposed to compensate the mutual coupling effect. To achieve a high performance current control, a feedback linearizing current controller is proposed to linearize and decouple the current control loop. A gain scheduling scheme is proposed to adapt the varying parameters in the mathematical model. The experimental results show that the proposed torque controller is suitable for low speed as well as for high speed.

## **Sliding Mode Control**

Because the SRM magnetization characteristics is highly non-linear, the torque is a complex and coupled function of the phase current and rotor position. It is difficult to find a current reference by analysis and the mathematical model is required to be accurate which is hard to obtain in practice. Sliding mode control is robust to model inaccuracies, thereby significant interest on variable structure systems and sliding mode control have been generated among researchers and application engineers in recent decades. The most salient feature of the sliding mode control is the existence of the motion in selected manifolds in state space [21]. Such motion results in a system performance that includes disturbance rejection and insensitivity to parameter variation[22]. The efforts to apply sliding mode control to switched reluctance motors can be found for variable speed SRM drive system can be found in many papers[23, 24, 25].

The sliding mode control for SRM torque ripple minimization was first proposed by Buja[26] in 1993. The sliding mode control is divided into two parts, one dealing with the current limitation and the other with the speed control. However, the motor is assumed working in the linear region of its magnetic characteristics.

In [27, 28], sliding mode torque control is formulated to minimize the SRM torque ripple. Experimental results are provided to prove the effectiveness of the torque control scheme. The sliding surface of the torque controller is defined by

$$\sigma(\theta, \omega, i) = T_e(\theta, i) - T_{ref} \quad (1.1)$$

By Lyapunov second method,  $\frac{1}{2} \frac{d}{dt} \sigma(x)^2 < 0$ , the control voltage is given to keep the system in sliding surface. In other words, if the voltage is applied to the phase, the torque error will be forced to zero.

In [29], the sliding mode flux linkage controller for torque ripple minimization, because the author believe that a flux linkage controller can easily incorporate the limitations imposed by the DC-link voltage and rotor speed, when calculating the torque reference required for constant torque operation. W.Shang *et al.* [30] presented a sliding mode flux-linkage controller with integral compensation for SRM. The controller is not model-based, avoiding the complexity of mathematical modeling and is easily implemented. Experimental results demonstrate that the proposed controller performs better and can be used as an alternative for nonlinear SRM drive systems.

### 1.2.3 Intelligent Control

Intelligent control is inherently a non-linear control with strong self-learning ability and adaptability. Therefore, it could be an ideal candidate to solve the control strategies of

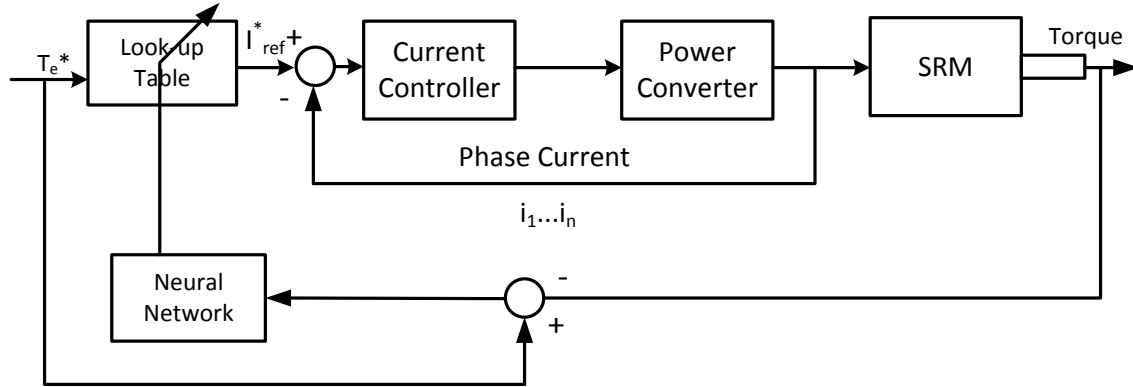


Figure 1.4: Neural Network Controller for SRM Drive

an inherently nonlinear system. By off-line learning on on-line learning with optimized performance index, the intelligent controller can reduce the torque ripple and realize high performance control to SRM.

## Neural Networks

The switched reluctance motor is a high non-linear system. The phase current, rotor position and overlap angle all contribute to the high torque ripple. The  $T - i - \theta$  model of the switched reluctance motor is hard to model and thus the torque is hard to control under different circumstances.

Using neural network to reduce the torque ripple is earliest proposed by Reay, *et al.*[31, 32]. The current profile is obtained with on-line learning to minimize the torque ripple. This method has the advantage of accounting for the effect ignored by the magnetic interaction between simultaneously conducting phases, windage and friction. The disadvantage for this method is that a torque sensor is required in the learning phase. Due to the large on-line computation, the transient response is degraded with this method and instability may occur if initial current is not properly set.

O'Donovan *et al.* solve those problems mentioned above by a neural network controller with off-line learning [33]. The learning process uses back propagation steepest descent algorithm. The torque can be estimated by the artificial neural network which eliminate the necessity for the torque sensor.

Shang,Reay and B.Williams[34], proposed a learning rated functions in CMAC neural network to control the torque ripple. The proposed method modifies the conventional LMS algorithm using a varying learning rate which is defined as a function of the rotor angle.

Lin *et al.*[35] used a B-spline neural network to control the torque ripple. The phase current profile can be obtained on-line in real time due to the local weights updating algorithm of the BSNN. Therefore, a good dynamic performance can be obtained by this control scheme.

In [36, 37], Rahman and Fahimi *et al.* used neural network to obtain a optimized instantaneous torque and mitigate the acoustic noise and vibration in switched reluctance motor. Difference from previous work using the static test data for learning, the learning data is generated from a dynamic SRM model. Hence, the control scheme has good performance even during the transient of the motor. Besides, the torque control scheme is optimized with maximum torque per ampere as the performance index.

Rahman *et al.*[38] proposes a control scheme for all operational regimes using neural network. There is a small table in the controller to identify the base speed for different torque demands. The base speed is to determine if the controller is going to work under high speed mode or low speed mode. The disadvantage of this control scheme is that under high speed, the motor is actually working at single pulse mode control, the current profile is not being controlled. Therefore, the torque ripple is still large due to the lack of current control.

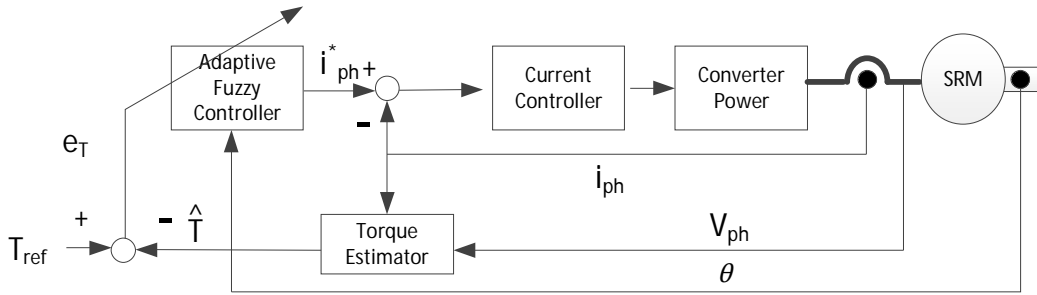


Figure 1.5: The adaptive fuzzy controller for torque control of SRM

## Fuzzy Control

Fuzzy control is one of the appropriate approaches for torque ripple control in SRM. Fuzzy logic controller is applied to SRM drive in [39, 40] for variable speed system. The SRM with fuzzy controller is robust to the inaccurate parameter and different operating conditions.

The torque ripple reduction using fuzzy logic was mentioned in [41] by Mir *et al.*. The rotor position is the input of the fuzzy controller, the phase current reference is the output. By revising the membership function to obtain an optimized conduction angle and commutation angle. The control block diagram is shown in Figure 1.5.

The fuzzy logic torque ripple minimization technique is also presented in [42, 43, 44]. The simulation results are given, however, they show large torque ripple during commutation interval.

In order to obtain a high quality performance, the fuzzy control is always combined with neural network [45, 46] combines fuzzy control and neural network to make the controller adaptive to speed and load.

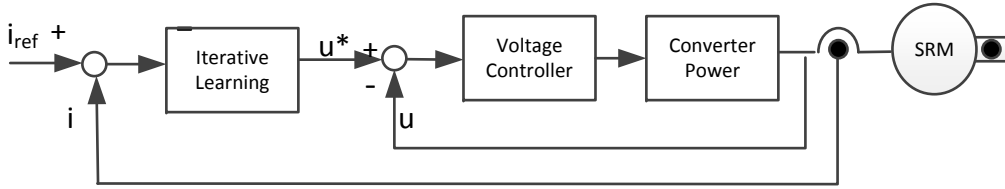


Figure 1.6: Block diagram for ILC-based current controller

### Iterative Learning Control

Iterative learning control is applied for constant torque control of switched reluctance motors. In [47, 48, 49], N.C. Sahoo developed a simple and efficient control algorithms for the constant torque control of switched reluctance motors. The approach consists of two distinct steps, i.e. determination of appropriate phase current waveforms for some specified torque and the subsequent generation of suitable phase voltage profiles for faithful tracking of these waveforms by the respective stator windings of the motor. This control scheme requires much less a priori knowledge of the magnetic characteristics. The block diagram for ILC-based current controller is shown in Figure 1.6.

The simulation and experimental results demonstrates the effectiveness of the proposed control scheme. However, due to the finite time required for ILC learning, there would be a performance degradation during transient periods. The paper [50] develops SMC for improving the control performance during transient periods and control the torque directly. The experimental results shows good performance of this control scheme.

The iterative learning control scheme doesn't need accurate  $T - i - \theta$  model for switched reluctance motor. It doesn't need much computation, hence it is a promising control method.

### 1.3 Challenges to SRM Torque Ripple Minimization

Previous torque ripple control methods had good control performance on the torque ripple attenuation during the conduction time. The torque can almost be controlled as a constant. However, the torque ripple happened during the commutation interval is not well solved. Due to the existence of the inductance for the switched reluctance motor, the current cannot jump from zero to a nominal value instantaneously, which gives rise to the tail current in the out-going phase and the delay in the coming phase. The phase current is impossible to have a good track to the reference. The TSF extended the commutation interval and defines various kinds of torque sharing functions to smooth the current reference, which gives a good performance at low-speed operation. However, in high speed, the back-EMF will be much larger than that in low speed operation, therefore, the current can not be produced very high and the reference current still have a steep rate which is hard for tracking. Hence, the torque sharing function is only suitable for low-speed application case.

The nonlinear control is one of the appropriate methods to control the torque ripple. The current controller may have a better performance compared to traditional PI control. However, the disadvantages are obvious. The switching frequency is varying which might exceed the switching speed ability. The chattering problem for sliding mode control needs extra efforts to be dealt with. The current reference generated still has large rate of change, hence, the high-speed operation is not suitable for this problem as well.

The intelligent control is inherently a non-linear control with self-learning, adaptability to model inaccuracy and uncertainty. With intelligent control, by training the network off-line or on-line, the output torque can reach constant regardless if the motor model is available or accurate. The current reference is given by the intelligent controller by learning and tuning the weights or membership functions in the controllers. The major disadvantage for the



intelligent control is that large amount of computation slows down the dynamic response.

## 1.4 ‘Pseudo-sinusoidal’ SRM

For all of these methods, adjacent phases are conducted during commutation interval with smoother phase current reference. With those methods, either the static SRM model is required, or a learning process is required in advance to obtain a current profile to design the reference current profile. Obtaining the SRM model and learning process all need large amount of time, and the rate of current is still relatively high. In such case, the SRM still has relatively large torque ripple at high-speed operation. The SRM application is limited in the high-speed field with smooth torque requirement. In 2012, a ‘psuedo-sinusoidal’ motor was proposed and designed by Dr. E. Swint in his dissertation [53]. This new switched reluctance motor has a phase inductance close to ‘sinusoidal’. A finite elementary analysis can be applied to this motor and obtain a current reference to eliminate the torque ripple. At this point, the process of obtaining the reference current doesn’t need the static magnetic model for the motor. Therefore, using this method, the inherent motor property is not investigated, eliminating the experiments measuring the motor model which are relatively troublesome and inaccurate.

## 1.5 Thesis Outline

Due to its cost advantage and ruggedness, the SRM is gaining much interests in the recent decades. However, due to its doubly salient structure, the SRM is known with large torque ripple which limits its use in places where high-quality control is required. The primary objective of this work is to present a new torque control scheme to minimize the torque

ripple, which is possible to be extended in high-speed application. This thesis consists of six chapters. The detailed outline is elaborated as follows.

Chapter 1 is the review of the background of switched reluctance motor and challenges to the torque ripple control. The switched reluctance motor is attracting more interests in industry and research institute due to its low-cost, ruggedness. However, available methods can only effectively control the torque ripple at relatively low speed. The primary object of this work is to present a new current control scheme which turns the high-quality high-speed SRM into possible.

Chapter 2 presents the basic operating principle of switched reluctance motor and the control of switched reluctance motor. The switched reluctance motor model is given and the torque generation principle is specified.

Chapter 3 presents the origin of the torque ripple in switched reluctance motor. An 'ideal' SRM with 'sinusoidal' inductance profile is used to obtain the reference current profile for simplicity. There are infinite current profiles which could give a constant torque. A current reference with minimum peak and rms value is chosen considering the efficiency. In this new control scheme, three phases are conducted during the whole operating period unlike the conventional method for which only two phases are conducted to coordinate the torque. The current reference is smoother compared to those in previous techniques, which implies this control scheme could be used to obtain a torque ripple free SRM in high-speed application. The current profile for a real SRM is given by finite elementary analysis. Simulation is given to prove the effectiveness of this method.

Chapter 4 presents the whole SRM drive system experimental setup. There are 4 major subparts to the whole system. The power state, current sensor, position sensor and the control part are specified separately in this chapter.

Chapter 5 presents the experimental results of the SRM drive system to prove the effectiveness of the new current ripple control scheme. The motor is operating under two different speed level. The torque ripple is relatively smaller compared with previous method although unknow low-frequency noise is shown in the results. Conclusions with the summary and the future work is presented in the final part.

# Chapter 2

## Operating Principle and Mathematical Model

### 2.1 Operating principle

The switched reluctance motor has significance differences compared with other conventional AC and DC motor. The torque is produced by the tendency of the moveable part to move to a position where the inductance of the excited winding is maximized. The structure of the switched reluctance motor is shown in Figure 4.5.

Different from traditional AC and DC machine, both the rotors and stators of the switched reluctance motor have salient poles, i.e. doubly salient poles structure. The rotors and stators are made of laminated steels. The stators have windings, while the rotors don't have. The number of the rotors and the stators are always different with each other to avoid zero start torque.

When current is flowing through phase C, the magnetic torque will attract the rotor to

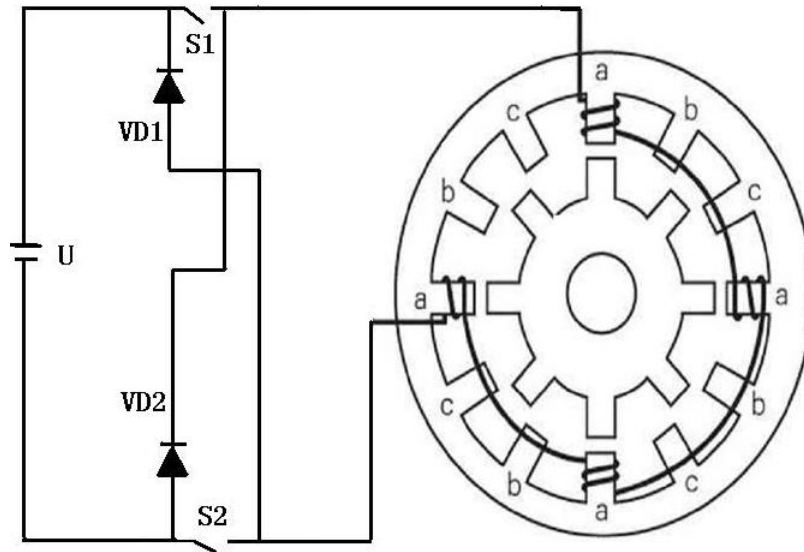


Figure 2.1: Structure of SRM

a position that is in align with the axis, making the phase C inductance at its maximum value. If the initial position is assumed as shown in Figure 2.1, exciting the phase in sequence  $A \rightarrow B \rightarrow C \rightarrow A$  will result in reversal of rotor rotation. Similarly, if the excitation sequence is  $C \rightarrow B \rightarrow A \rightarrow C$ , the rotor will rotate clockwise. Hence, it can be seen that the SRM rotation direction has nothing to do with the current direction, but it is determined by the phase winding excitation sequence. In practice, multiphase excitation control may be utilized to realize several special functions such as torque ripple minimization and maximum torque per ampere.

## 2.2 Switched Reluctance Machine Mathematical Model

### 2.2.1 Equivalent Circuit

According to Farady's law, the flux-linkage  $\Psi_k$  and voltage  $U_k$  for phase  $k$  during fluxing process can be expressed with[51]:

$$U_k = R_k \cdot i_k + \frac{d\Psi_k}{dt} \quad (2.1)$$

In this equation:  $U_k$  is the  $k$ th phase motor winding voltage;  $R_k$  is  $k$ th phase winding resistor;  $i_k$  is  $k$ th phase winding current;  $\Psi_k$  is  $k$ th phase flux linkage;

The flux can be described as the product of induction and current, namely,

$$\Psi_k = L_k(i_k, \theta) \cdot i_k \quad (2.2)$$

Combining equation (2.1)and equation (2.2) gives

$$U_k = R_k \cdot i_k + L(\theta, i_k) \frac{di_k}{dt} + \frac{dL(\theta, i)}{d\theta} \omega_m i_k \quad (2.3)$$

In this equation, the three terms on the right-hand side represent the resistive voltage drop, inductive voltage drop, and induced emf, respectively. The equivalent circuit is therefore given as Figure 2.2.

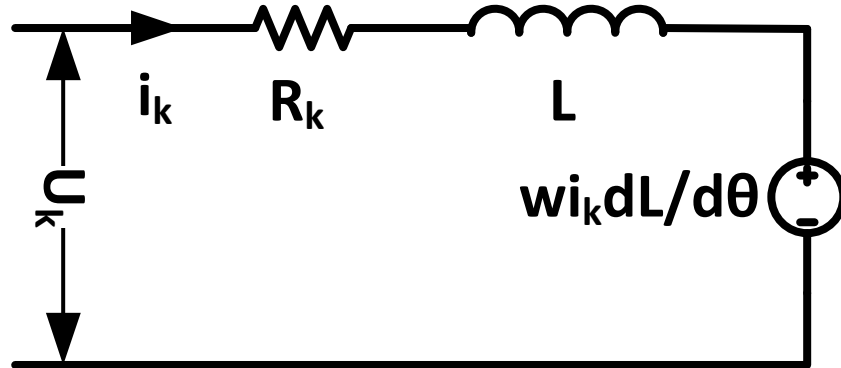


Figure 2.2: Equivalent Circuit for SRM

## 2.2.2 Torque Equation

The torque equation for the switched reluctance motor equals to

$$T_e - T_L = J \frac{d\omega}{dt} + B\omega \quad (2.4)$$

where  $T_L$  is the load torque,  $T_e$  is the electromagnetic torque,  $J$  is the rotor inertia,  $B$  is the friction constant.

## 2.2.3 Instantaneous Torque Generation

The instantaneous torque generating process can be explained by basic electromechanical conversion principle. The instantaneous torque expression derivation process is given in [51]. Here lists some of its important derivation. Note that some of the equation derivation in this subsection is given by [51].

As is shown in Figure 2.3, when current  $i$  is flowing through phase  $p$  at rotor position  $x$ , the

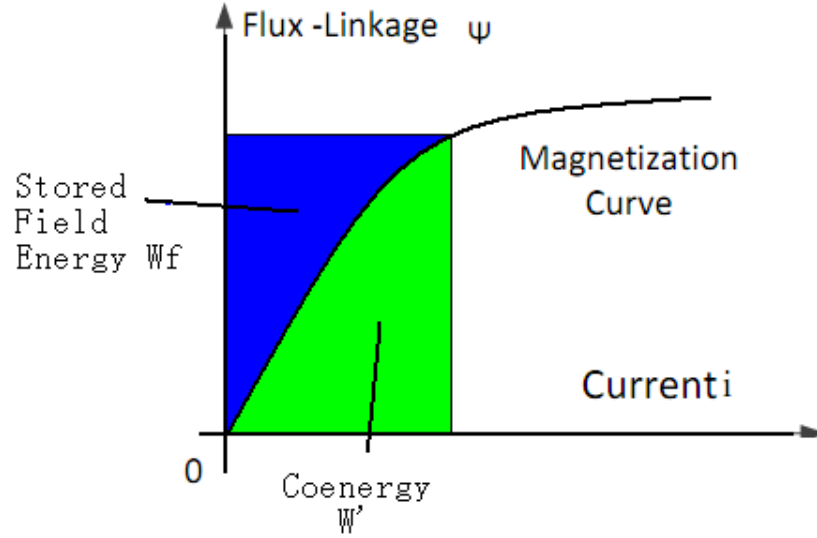


Figure 2.3: Torque Generation

stored field energy and the coenergy are defined by

$$W_f = \int_{\Phi_1}^{\Phi_2} F d\Phi \quad (2.5)$$

$$W' = \int_{i_1}^{i_2} \Phi dF \quad (2.6)$$

The stored field energy corresponds to the blue area, the coenergy corresponds to the green area. The electrical input energy is given by

$$W_e = \int e i dt = \int i dt \frac{dN\Phi}{dt} = \int N i d\Phi = \int F d\Phi \quad (2.7)$$

When there is no mechanical work, i.e. without rotor movements, the electrical input energy is equal to the stored field energy. The electrical input energy is also equal to the sum of the



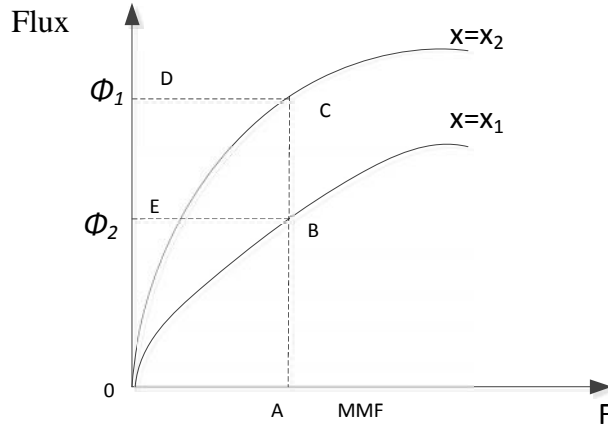


Figure 2.4: Flux VS MMF

stored field energy  $W_f$  and the energy  $W_m$  that is converted to mechanical work.

$$W_e = W_f + W_m \quad (2.8)$$

By this way, the electromagnetization and the mechanical work are connect to each other, the instantaneous torque can be given according to following derivation.

In order to derive the instantaneous torque at position  $x_1$ , an incremental changes on the rotor position  $\delta x = x_2 - x_1$  is considered. The incremental relationship between electrical input energy, stored field energy and mechanical work turns out to be,

$$\delta W_e = \delta W_f + \delta W_m \quad (2.9)$$

With Figure 2.4 and Equations (2.5-2.7) discussed above, the incremental energies are given by,

$$\delta W_e = \int_{\phi_1}^{\phi_2} F_1 d\phi = F_1(\phi_2 - \phi_1) = \text{area}(BCDEB) \quad (2.10)$$

$$\delta W_f = \delta W_f - \delta W_f = \text{area}(OCDO) - \text{area}(OBEO) \quad (2.11)$$

With Equation (2.9) , the incremental mechanical energy is derived as:

$$\delta W_m = \delta W_e - \delta W_f = \text{area}(OBCO) \quad (2.12)$$

which is the area between the two curves for a given magnetomotive force. In the case of rotating machine, the incremental mechanical energy in terms of electromagnetic torque and the incremental rotor position changes is given by,

$$\delta W_m = T_e \delta \theta \quad (2.13)$$

For instantaneous torque, it is assumed that the rotor position change is small, i.e.  $\delta x \rightarrow 0$ , the phase current can be considered constant. In this case, the incremental coenergy can be proved to be equal to the incremental mechanical work[1]. The coenergy can be written as,

$$W' = \int \Phi dF = \int \Phi d(Ni) = \int \lambda(\theta, i) di = \int L(\theta, i) i di \quad (2.14)$$

Since phase current  $i$  can be considered constant in this case,  $L$  is dependent only on rotor position  $\theta$ , which is in general not the case, the electromagnetic torque is given as,

$$T_e = \frac{\delta W_m}{d\theta} = \frac{\delta W'_f}{\delta \theta} = \frac{dL(\theta, i)}{d\theta} \frac{i^2}{2} \quad (2.15)$$

In this case, the phase inductance is only dependent on the rotor position, the phase current will have no impact on the phase inductance. However, this is rarely happened in switched reluctance motor operation, since the inductance will reduce due to saturation under large phase current. Ignoring the saturation, the flux vs current characteristics is plotted in Figure 2.5

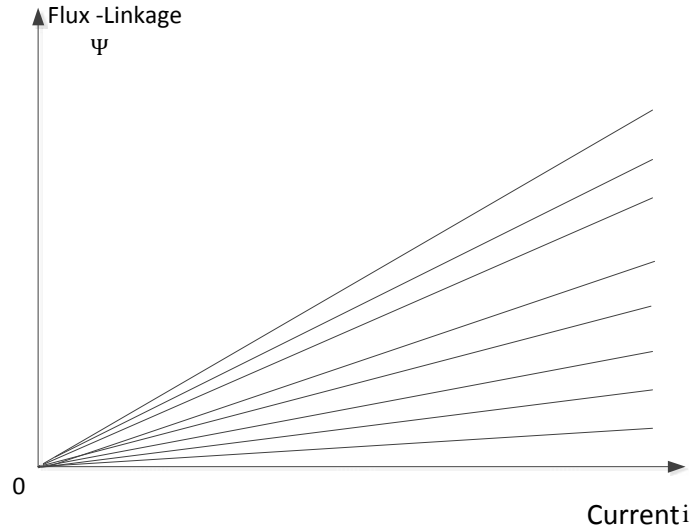


Figure 2.5: Linearized Magnetic Characteristics for SRM

### 2.2.4 Idealized Induction Model

From Equation(2.15), it can be seen that in order to get instantaneous torque,  $\frac{dL(\theta,i)}{d\theta}$ , must be given. This subsection gives an idealized induction model in one phase of switched reluctance motor at a constant current. In this idealized induction model, several assumptions are made to simplify the analysis.

- (1) Ignoring the magnetic saturation, the inductance is independent of winding current.
- (2) Ignoring the magnetic nonlinearity and magnetic fringing effect
- (3) Ignoring the magnetic hysteresis loss and eddy current loss
- (4) The converter switches are ideal switches, the switch function is completed instantaneously.
- (5) the motor runs at constant speed
- (6) the power supply gives constant input voltage.

Due to its doubly salient pole structure, the induction varies with respect to different rotor position. The maximum inductance reaches when the rotor is at the aligned position where the rotor poles is exactly aligned with the stator poles. The minimum inductance reaches

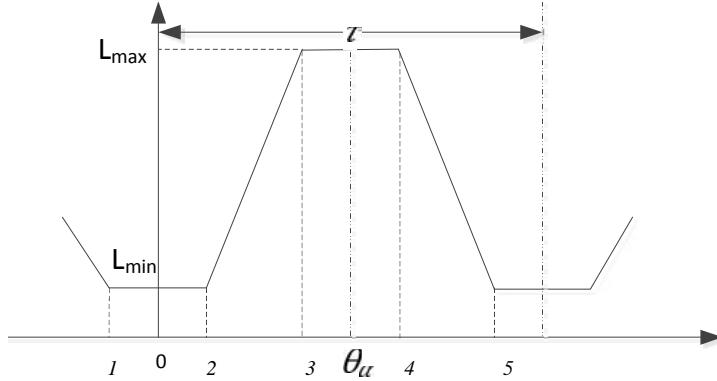


Figure 2.6: Phase Inductance VS Rotor Position

when the axis of the rotor is aligned with the poles of the stator. The phase inductance variation within one period of rotor position is shown in Figure 2.6. According to Figure 2.6 and Equation 2.15, it can be seen that the switched reluctance motor can operate in 4 quadrant. From Equation 2.15, the torque direction is just dependant on  $\frac{dL}{d\theta}$ , the current direction has no effect to the torque. If the phase is conducted during  $\theta_2 \leq \theta < \theta_3$  interval, since  $\frac{dL}{d\theta} > 0$ , the motor is at motoring mode. Part of the electrical input energy is converted to mechanical work, while the left energy is stored in the coil as stored field energy. If the power supply stops offering energy during this interval, some of the stored energy will be converted to mechanical work, the other will be feedback to the power source. There is still going to be a positive torque. If the motor is conducted with current at interval  $\theta_3 \leq \theta < \theta_4$ , the energy will be feedback to the power source, there is no torque on the motor. If the phase is conducted with current between interval  $\theta_4 \leq \theta < \theta_5$ , because  $\frac{dL(\theta)}{d\theta} < 0$ , there will be negative torque production, i.e. the braking torque. The mechanical energy is converted to electrical power to the power source and the part of field energy is feedback to the torque. The switched reluctance motor is working as a generator.

From above analysis, it can be seen that the current profile need to be designed in order to get desired torque value and smooth torque profile to reduce the mechanical wearing

and acoustica noise. The next section will discuss about the control of switched reluctance machine.

## 2.3 Control strategy

There are various kinds of switched reluctance motor control method, such as the the phase voltage,  $u_k$ , the phase current  $i_k$ , firing angle  $\theta_{on}$  and commutation angle  $\theta_{off}$ , etc. There are three methods to control those controllable parameters, angle position control, current chopping control, chopping voltage control.

### 2.3.1 Single Pulse Operation

Single pulse operation is to switch the supply voltage on at the turn-on angle  $\theta_{on}$ , and switch off at the commutation angle  $\theta_{off}$ . The 'turn-on' angle locates where the induction is small with small back-EMF. The current will go up very fast, reaching to a large value in a short time. When the rotor arrives at  $\theta_2$ , where the induction starts increase and current stop increasing. Hence, smaller 'turn-on' angle will generage larger torque. However, the current would be too large if  $\theta_{on}$  is too small due to longer current increasing time. Hence, the 'turn-on' angle should be chosen at reasonable range. The current waveform corresponding to different 'turn-on' angle is shown in Figure 2.7.

The commutation angle locates where the induction is large and the back emf large. The current doesn't have large variation. Hence, tuning  $\theta_{off}$  would not have great impact to the current value. The commutation angle should be chosen to generate large motor torque while reducing the brake torque. The current waveform corresponding to different current waveform is shown in Figure 2.8.

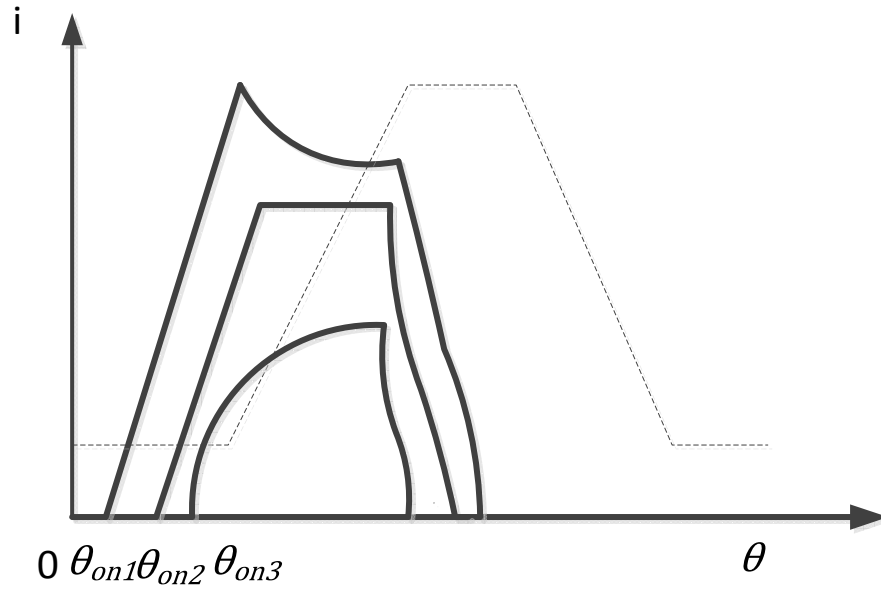


Figure 2.7: On-Angle for Single Pulse Operation

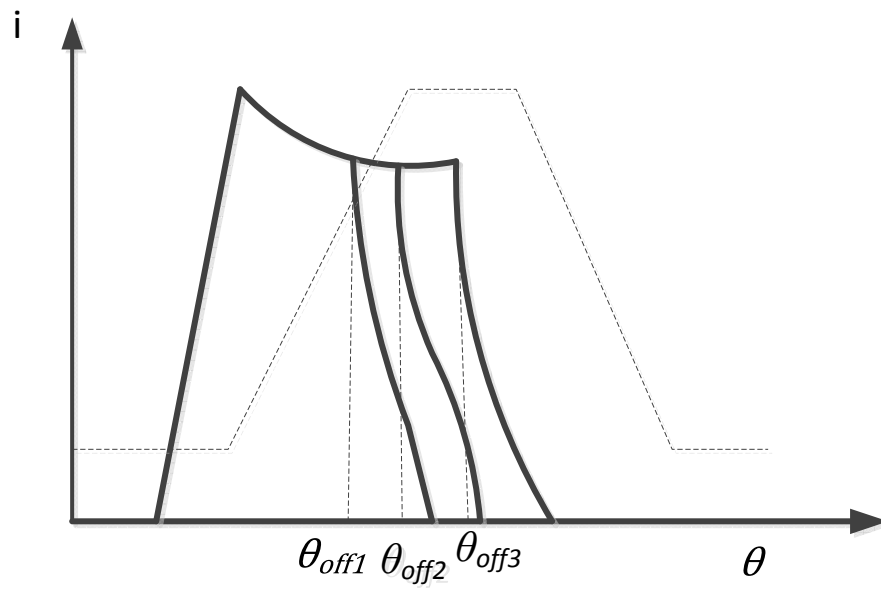


Figure 2.8: Off-Angle for Single Pulse Operation

In sum, the angle position control has following characteristics,

(1) wide range torque adjustment. Under single pulse control, the current can be present from 0 to the whole period. (2) Multiple phase conduction. When there are more phase conducted, the motor has larger torque, the torque ripple will be smaller. When the load varies, it could be realized by increasing or decreasing the conducting phase correspondingly. (3) The disadvantage of the single control is that it is rarely used in low speed application. The peak current is always controlled by emf. When the speed is low, the emf is small, hence the current in the motor is going to be very high. Additional current limit needs to be added, hence the angle position control is typically used in high speed application case.

### **2.3.2 Voltage Chopping Control**

Keeping the firing angle  $\theta_{on}$ , commutation angle  $\theta_{off}$  unchanged, making the power switches under pwm modulation mode. By regulating the pwm duty cycle, the average voltage is changed as well as the phase current. Increasing the frequency will smooth the current waveform out, reduce the acoustic noise, but the switches need to be able to work under the fast switching frequency.

### **2.3.3 Current chopping control**

When the motor is operating at low speed or at start-up process, the phase current is usually very large because there are not enough impedance and back-EMF. The current chopping control is always utilized to limit the large instantaneous current so that they won't destroy the power transistors or the motor. The method is to limit the current within a hysteresis band.

The current chopping control embodies several advantages: (1) The current chopping control

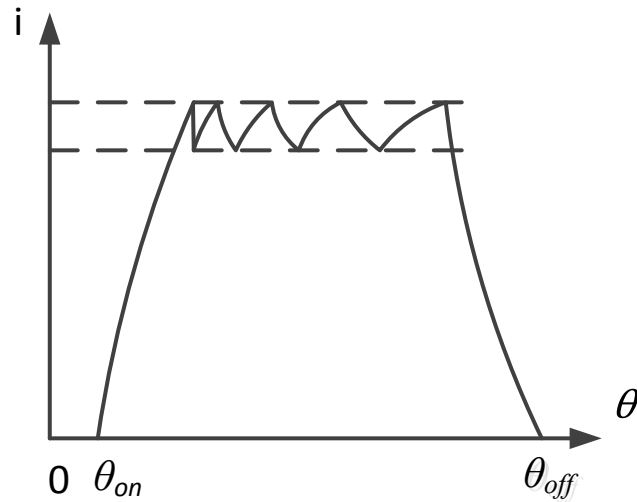


Figure 2.9: Current Chopping

will protect the power transistors and the motor from large instantaneous current because the current is limited to a band. It is always utilized in low speed operation and braking mode. (2) The torque obtained by the current chopping control is smooth compared with other two method. It is usually utilized in the torque control system by current profiling. The disadvantage for current chopping control is that it has slow response to the load variation. Since, the current within the motor is limited to a fixed value, when the load varies, the current cannot be enough to provide enough torque to regulate the speed variation due to the load change.

## 2.4 Variable speed Control for Switched Reluctance Motor Drive

Figure 2.10 shows the block diagram of the switched reluctance motor connected to a load with closed loop speed control. The speed error is processed through a proportional plus



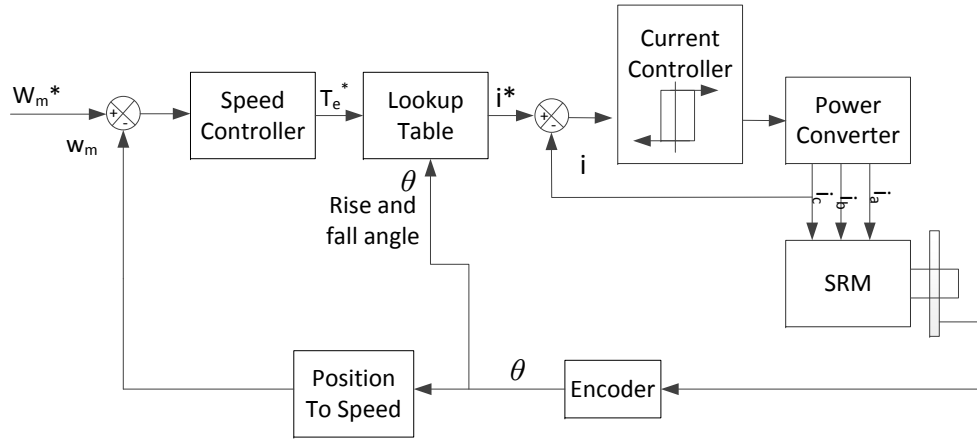


Figure 2.10: Variable Speed Control System

integral (PI) controller and a limiter to yield the torque command  $T_e^*$ . From the torque command, the current command  $i^*$  is obtained. This torque constant is for the linearized inductance vs. rotor position characteristics for a particular value of current. The current command is added and subtract from the hysteresis window,  $\Delta i$ , to obtain the  $i_{max}$  and  $i_{min}$  that determine the switching of the phase and main switches of any converter. The currents are injected into respective windings based on their position information obtained from an encoder or a resolver or position estimator. The rise and fall angles are calculated from the magnitude of the stator current, rotor speed and minimum and maximum inductances. The rise and fall angles are incorporated with the rotor position information in the switch control signal generator block shown in the block diagram.

### 2.4.1 Summary

In this chapter, the operating principle of switched reluctance motor was discussed. The rotor tends to move to a position where the inductance of the excited winding is maximized. The mathematical model is given as a preparation for the next step: control of the switched reluctance motor. The torque generation mechanism is introduced here. Ignoring

the nonlinearity and magnetic saturation, the instantaneous torque is equal to  $\frac{1}{2} \frac{dL(\theta)}{d\theta} i^2$ . The instantaneous torque expression is used in the next chapter for current profiling to realize ripple free torque control. Finally, the SRM control strategy is briefly introduced at the end of the chapter. There are two control strategies for SRM. The single pulse control, voltage chopping and current chopping. In high speed operation, single pulse control is used. By changing the turn-on angle and turn-off angle, the speed can be changed. The current chopping is used to control the SRM torque, which is typically used in a high-quality SRM drive system.

# Chapter 3

## Torque Ripple Minimization in SRM

This chapter introduces a new current control scheme for SRM torque ripple minimization. A new reference current profile is obtained using trigonometric identities for an idealized SRM with a ‘sinusoidal’ phase inductance. If the SRM phase current is well-controlled to follow the reference, the torque ripple would be eliminated and the bus current ripple disappears. As a result, the acoustic noise is reduced and the need for the failure-prone electrolytic capacitor is released. However, there are some deficiencies for ideal ‘sinusoidal’ SRM, a ‘pseudo-sinusoidal’ SRM is proposed to solve these problems. A current control scheme to minimize the torque ripple for ‘pseudo-sinusoidal’ is investigated accordingly. MATLAB simulation and experiments are conducted for both the idealized inductance SRM and the ‘pseudo-sinusoidal’ SRM to verify the effectiveness of the new SRM torque control algorithm.

### 3.1 Origin of Torque Ripple in SRM

Due to its doubly salient pole structure, the torque ripple is much larger compared with traditional AC and DC machines. The nonlinear and discrete torque production mechanism

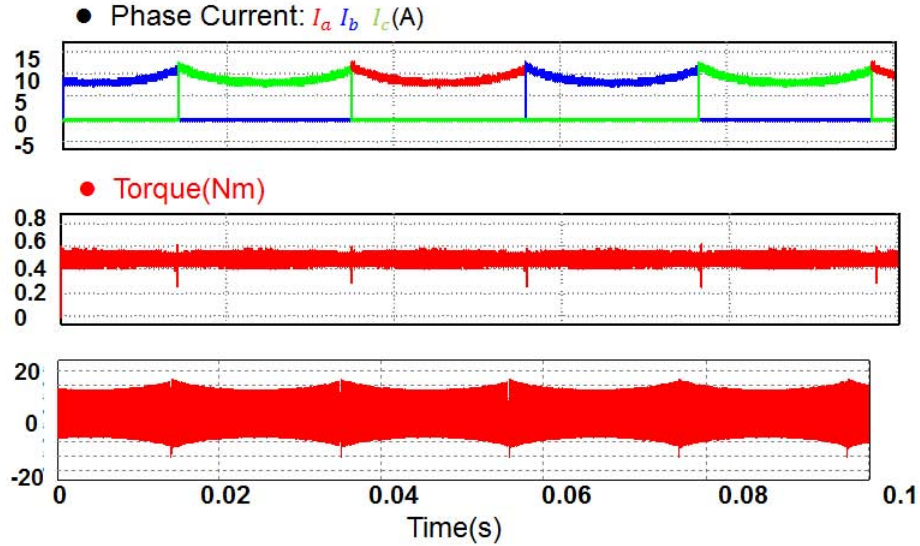


Figure 3.1: Torque Ripple Generation

in the motor proves to be another reason for high ripple in the torque. The origin of the torque ripple is shown in Figure 3.1.

Figure 3.1 shows a traditional SRM torque control strategy. Each time, there is only one phase excited with phase current. At the commutation point, the outgoing phase current dropping from nominal value to zero and incoming phase current rising from zero to nominal value instantaneously. The current reference is calculated with the inverse of the torque generation function.

$$i^* = \sqrt{\frac{2T_e}{dL/d\theta}} \quad (3.1)$$

Hence, the current reference for each phase is a series of current pulses as shown in Figure 3.1. If the current is well controlled by the current controller to follow the reference, the total output torque is going to be a constant. However, in practice, an infinite fast controller does not exist to track a discrete current reference without any overshoot  $OS\%$  and transition time  $T_s$ . From Physical point of view, the current can not change from zero to its nominal value instantaneously with an inductor present in the circuit. Hence, there is always discrepancy

between the real current and current reference at the commutation interval, which would lead to torque pulsations at the commutation interval. As is shown in Figure 3.1, although the current reference can be tracked very well during each phase conduction period, at the commutation interval  $t=0.035$ , the phase current b cannot drop to 0 instantaneous, and the current in phase c cannot rise to the reference value without any delay. Hence, at this commutation time, phase b and phase c are conducted simultaneously, the total torque is the sum of individual torque. Hence, the output torque at this time would deviate from its reference value. The torque ripple could be very large. As is shown in the case Figure 3.1, the torque ripple reaches about 40%, which is intolerable for servo system.

Assume the SRM is operating at constant speed. The output power is equal to  $P_{out} = T_e\omega$ . The fluctuating torque value will result in the fluctuation of the output power. Ignoring the power loss, namely, the input power  $P_{in} = Ui$  is equal to the output power. The output power is vibrating, the input voltage is a constant, hence the bus current will vibrate, in response to the torque ripple at the commutation interval.

The torque ripple will introduce shaft speed vibration and acoustic noise to the system, as well as considerable current ripple at the bus for which large electrolytic capacitor is used to attenuate it. However, the electrolytic capacitor is of low reliability, which will reduce the system stability and increase the volume of the inverter. The excessive torque ripple has limited the SRM applications in servo applications. There are two approaches for torque ripple application. One method is to reduce the torque dips by stator and rotor shape optimization. The other method is to use electrical control method to coordinate current in different phases to reach a constant output torque. In this aspect, the torque control is essentially a current control.

Several method has been proposed to minimize the torque ripple in SRM, such as torque sharing function method, neural network, fuzzy control. The effectiveness of these meth-

ods have been proved by experimental results with relatively good performances. In [52], G.Dunlop propose a current profile for a four phase switched reluctance motor with ‘sinusoidal’ phase inductance. Each time, two adjacent phases are conducted with current, the square of which profile is a ‘sinusoidal’ waveform. Mathematically, the output torque would reach to constant value. Current ripple is therefore eliminated. However, the proposed method can only be applied to a four phase switched reluctance motor. This paper extends this current control scheme to a three-phase switched reluctance motor.

## 3.2 New Torque Minimization Control Scheme

Traditionally, the motor inductance shape is like trapezoidal profile. Torque sharing method is utilized to attenuate the torque ripple, where during the commutation interval, two phases are conducted with current controlled to a desired profile. The output torque during the commutation interval can be a constant with this torque coordination between two phases. This section proposes a new approach in which the motor inductance is modeled as a ‘sinusoidal’ profile. By utilizing the trigonometric identities, the torque can be constant without any phase commutation ripple, since the current reference is smooth enough for tracking. Before introducing the new torque control scheme, it is necessary to make several assumptions:

- (i) The magnetic saturation is ignored, which means that the inductance is independent on the phase current, the magnetization curves are a cluster of straight lines. However, in practice, this is not the case;
- (ii) The mutual inductance in the motor is not considered;

A three-phase motor new torque control scheme is discussed below. The output electromagnetic torque is equal to the sum of the individual torque for an  $n$  phase SRM control system.

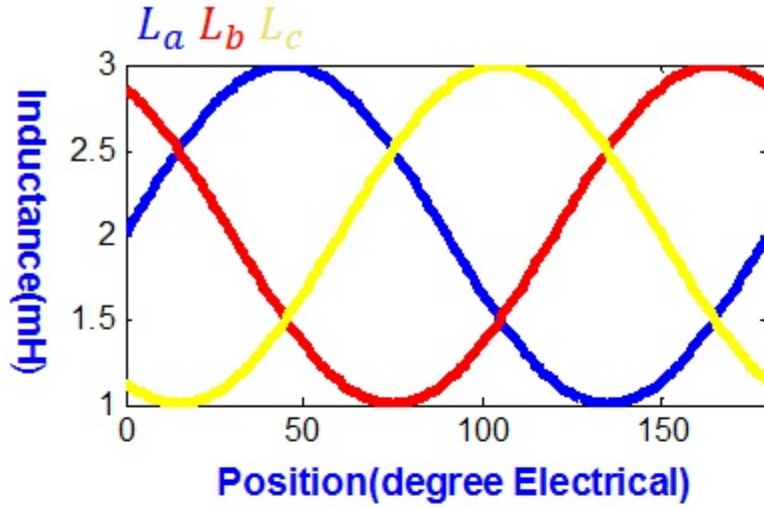


Figure 3.2: Inductance Profile

Assume that the SRM has symmetric three phase ‘sinusoidal’ inductance, with trigonometric identities, the current references in three phases can be derived respectively, as a result of which, the sum of the individual torque will reach to a constant value. The mathematical derivation process is presented as below.

Suppose the three-phase SRM has following ‘sinusoidal’ inductance defined by Equation 3.2

$$\begin{cases} L_a = L_{a0} + L_{a1} \cos(2\theta - \phi) \\ L_b = L_{b0} + L_{b1} \cos(2(\theta - 120) - \phi) \\ L_c = L_{c0} + L_{c1} \cos(2(\theta + 120) - \phi) \end{cases} \quad (3.2)$$

The three phases switched reluctance motor is symmetric for each phase parameters, hence,

$$L_{a0} = L_{b0} = L_{c0} = L_0, L_{a1} = L_{b1} = L_{c1} = L_1 \quad (3.3)$$

An example is shown in Figure 3.2, If the phase current is given by Equation 3.4

$$\begin{cases} i_a = \sqrt{I_0} \sqrt{\frac{1}{2L_{a1}} - \frac{1}{2L_{a1}} \sin(2\theta - \phi)} \\ i_b = \sqrt{I_0} \sqrt{\frac{1}{2L_{b1}} - \frac{1}{2L_{b1}} \sin(2(\theta - 120) - \phi)} \\ i_c = \sqrt{I_0} \sqrt{\frac{1}{2L_{c1}} - \frac{1}{2L_{c1}} \sin(2(\theta + 120) - \phi)} \end{cases} \quad (3.4)$$

The individual torque can be calculated respectively by Equation 2.15. The instantaneous total output torque is equal to the sum of the instantaneous individual torques. With the inductance profile expression and the given phase current reference, the total instantaneous torque can be calculated as following,

$$\begin{aligned} T &= T_a + T_b + T_c \\ &= -I_0 \sin(2\theta - \phi) - I_0 \sin(2(\theta - 120) - \phi) - I_0 \sin(2(\theta + 120) - \phi) \\ &\quad + I_0 \sin^2(2\theta - \phi) + I_0 \sin^2(2(\theta - 120) - \phi) + I_0 \sin^2(2(\theta + 120) - \phi) \\ &= 1.5I_0 \end{aligned} \quad (3.5)$$

From Equation 3.5, it can be seen that, corresponding a ‘sinusoidal’ inductance profile, if the current can be able track the calculated reference as is given by Equation 3.4, the output torque is going to be constant.

Simulation is built to verify the effectiveness of the new ripple free torque control scheme. The simulation is conducted with PSIM and SIMULINK co-simulation environment. The MATLAB is responsible for the control loop and the PSIM is responsible for the power stage. The simulation circuits are shown in Figure 3.3 and Figure 3.4. In this simulation, the motor is a three phase SRM with 12 stators and 16 rotors. The phase inductance is the fourier curve fitting for a real SRM phase inductance. The individual phase inductance is given as,

$$L(\theta) = a_0 + a_1 \cos(2\theta) + b_1 \sin(2\theta) \quad (3.6)$$



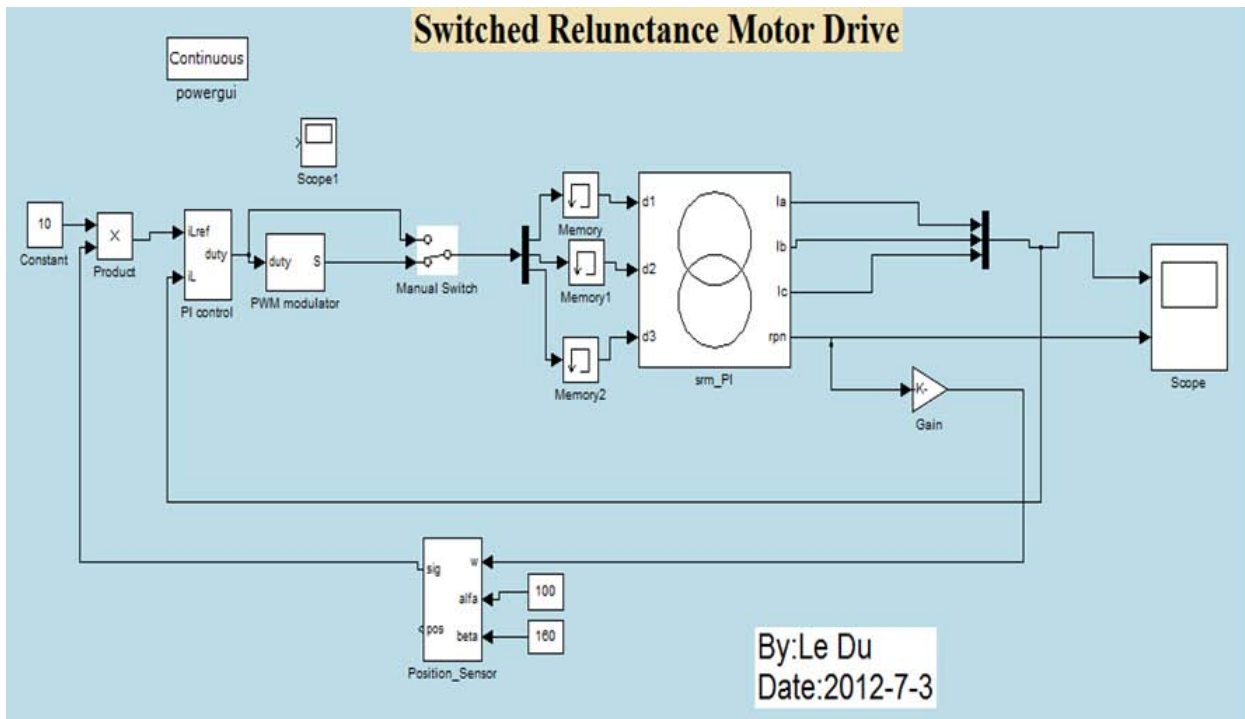


Figure 3.3: MATLAB Simulation Schematic

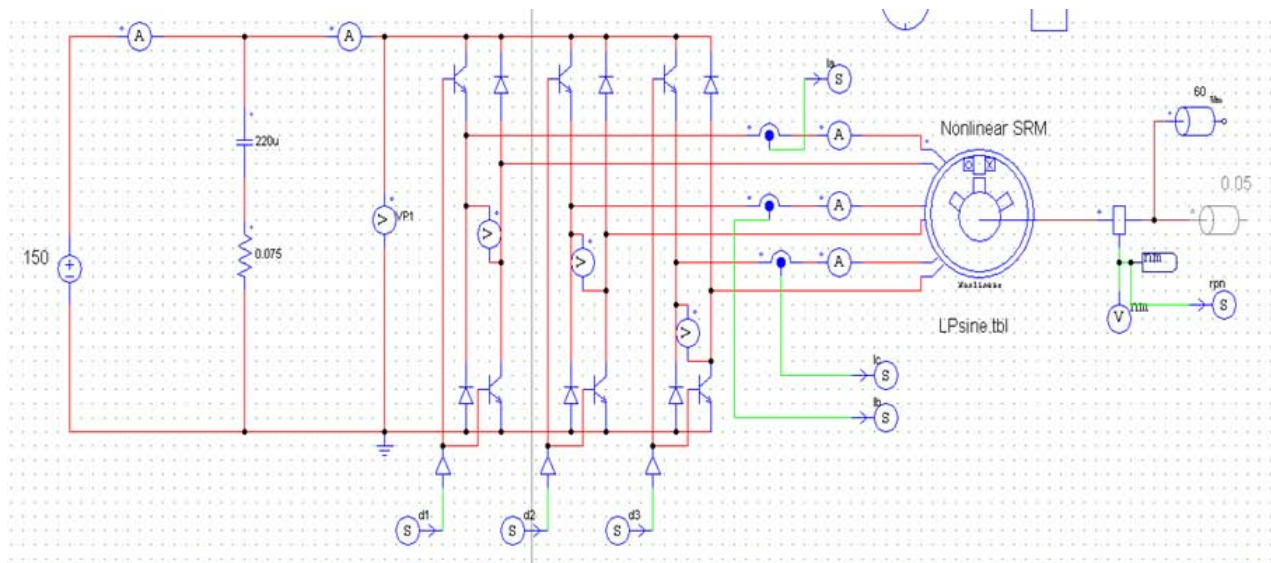


Figure 3.4: PSIM Simulation Schematic

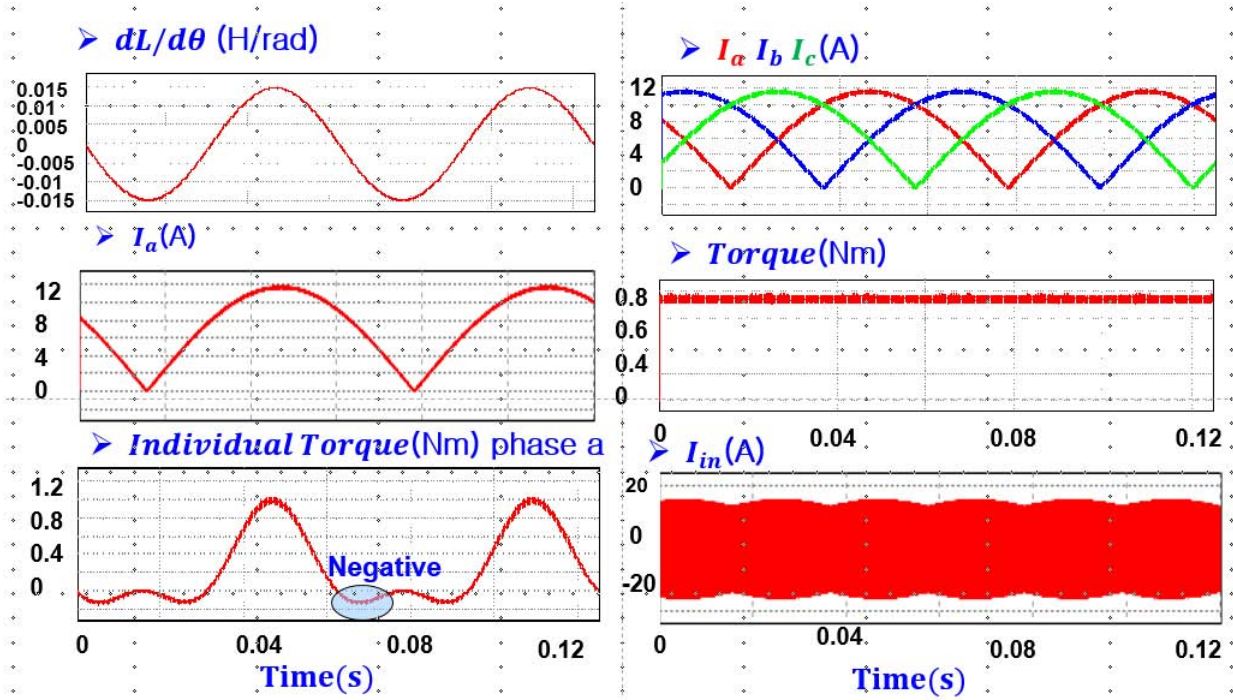


Figure 3.5: Simulation of the New Current Control Scheme

where  $a_0 = 0.002513$ ,  $a_1 = 0.0009107$ ,  $b_1 = -0.0001037$ . The motor drive system is controlled with PI control with modulation frequency at 10kHz. All the power switches are considered as ideal switches, the switch on and off can be finished instantly. The motor is operating at constant speed of 60rpm. The input voltage of the system is 150V. The simulation result is shown in Figure 3.5. From the simulation result, it can be seen that for ideal ‘sinusoidal’ inductance SRM, the torque ripple can be controlled to zero. The input current still exhibits a large current ripple, however, the current ripple during the commutation interval is eliminated.

Compared with traditional control method, the new torque ripple control scheme is different with the previous approach. For conventional control method, each time, there would be less

than 2 phases conducted to coordinate the torque for a three-phase SRM. The individual torque at each phase conduction time would be a constant, multiphase excitation is only utilized at the commutation interval. The system needs a commutation controller to decide the firing angle and commutation angle to open or switch off one phase. The proposed new control scheme is quite different with traditional control concept. All the three phases are conducted during all the SRM operating time. Hence, the firing angle and commutation angle concept is eliminated. The commutation controller is no long used under the new current control scheme.

From the simulation result, it can be seen that the torque ripple and current ripple happened at the commutation interval are eliminated. Different from traditional discrete current reference, the new proposed current reference is continuous, which can be tracked with well-designed current controller without any overshoot and transition time. The new control method overcome the discontinuous current tracking problem, hence torque ripple and current ripple are eliminated.

There are still very large current ripple shown in the simulation result. The current goes from positive to negative value on the input side before the input capacitor. This phenomenon could be explained as follows. The current in each SRM phase is a positive value with little high frequency ripple at switching frequency because it is well-controlled by the current controller. However, looking from the input side for each phase, the input voltage jump to positive value when IGBTs are on, and jump to negative value when the diodes are on. The voltage vibrate violently at the switching frequency. Reflected on the power, it has very large ripple. However, at the power source, the output voltage is constant. Ignoring the loss of the motor drive system, the power at each point should be same. Hence, the input current will have very large ripple although its average value is constant. Changing the circuit topology may be a solution to the current ripple, but it is not discussed in this paper.

Note that there are other current reference that can realize constant torque other than current reference given by Equation 3.4. It can be proved that the first term under the square root can be any value, which means that the first time under the square root of each expression in Equation 3.4,  $\frac{1}{L_{a1}}, \frac{1}{L_{b1}}, \frac{1}{L_{c1}}$  can be any value as long as

$$\begin{cases} A - \frac{1}{2L_{a1}} \sin(2\theta - \phi) > 0 \\ B - \frac{1}{2L_{b1}} \sin(2(\theta - 120) - \phi) > 0 \\ C - \frac{1}{2L_{c1}} \sin(2(\theta + 120) - \phi) > 0 \end{cases}$$

However, a smallest value is chosen as  $A = \frac{1}{L_{a1}}, B = \frac{1}{L_{b1}}, C = \frac{1}{L_{c1}}$  for saturation consideration, because the motor tends to enter the saturation region as the current increases. Another reason to use the smaller current is to reduce the conduction loss with smaller rms current in efficiency consideration.

The idealized ‘sinusoidal’ SRM does not exist in the real world. In practice, the phase inductance is close to a sinusoidal profile, not an exact one. Finite element analysis can be utilized to calculate a current reference for this kind of pseudo-sinusoidal SRM(PSSRM). However, the previous derivation and results still have some value. It could be a design guide line for motor design or motor drive engineer when they design the SRD system in following aspects:

First, the magnitude of phase-n current is equal to

$$I_n = \sqrt{\frac{T_0}{2L_{n1}}} \quad (3.7)$$

Since the magnitude of phase-n inductance is determined by motor design,  $I_0$  is the only parameter that can be used to change the output torque. In order to get a desired torque

$T_0$ , the magnitude of the current inject to phase n can be estimated by above Equation 3.7. The output torque is proportional to the square of the current magnitude, which means that changing the magnitude of the phase current will have great effect on the output torque value.

Second, Equation 3.4 gives the current reference position information corresponding to the rotor position. This will give engineer an information where to place the current profile with respect to the rotor position.

Third, Equation 3.7 also reveals a relationship between inductance and the the output torque for motor design engineer. The greater the inductance magnitude of the motor, the greater output torque under a fixed phase current value. If the difference between maximum inductance and minimum inductance is small, more current is needed to get a desired output torque.

There are also some disadvantages for this new proposed method. The conduction loss could be increased, because three phases are conducted with current at the same time. The conduction loss could be larger compared with conventional control method. Another disadvantage is that as constant output torque is reached, the motor cannot operate with its largest output torque, which means the average torque is decreased by torque minimization. As is shown in the simulation result, there are some negative region for individule phase torque to coordinate with other individual phase torques to reach a constant.

However, in practice, there is no exact sinusoidal machine. Considering the saturation effect, the inductance of the switched reluctance machine is even more complex. Most of the switched reluctance motor inductance profiles are modeled as trapezoidal profile.

In 2012, a pseudo-sinusoidal machine was proposed and designed by Dr. Ethan Swint in his dissertation and a paper[53, 54]. In the paper, E.Swint *et al* points out that the motor

would suffer voltage saturation if the current profile is the one discussed in [54]. Similarly, if the current profile is the one derived in Equation 3.4, the voltage saturation would happen again due to the step change of the rate of current. The voltage would have a step response with some overshoot or delay, therefore, there would be some negative effect on the current loop. The motor proposed by Dr. E.Swint revise the inductance profile so that it is like a ‘sinusoidal’ waveform, not a pure one, so that the rate of current reference would not have a step change, eliminating the voltage saturation problem. The motor was designed by finite elementary analysis. By shaping the stator and rotor profile, the inductance profile of the switched reluctance motor is close to the ‘sinusoidal’ waveform, but not an exact one. In this case, the current profile is obtained by Finite Elementary Analysis. The mathematical analysis in this section still gives us valuable information as mentioned above. Curve fitting can be utilized to get an approximate current profile by mathematical derivation, and then set it as initial value of the iteration process for the finite elementary analysis to save the computation time.

### **3.3 Implementation for Pseudo-sinusoidal SRM**

The switched reluctance motor designed in [53, 54] is a three-phase motor with 12 stators,16 rotors. The individual phase inductance is shown in Fig 3.6. The phase inductance varies from 1.5mH to 3.5mH. With finite elementary analysis, the current profile is given as Figure 3.7.

With this current profile, the torque ripple derived by finite elementary analysis reach to 9.54 % by simulation. The simulation result of the system is shown below in Figure 3.8.

In this simulation, the motor is operating under constant speed load with 60rpm, with 150 V input and ideal switch without any switching time. The saturation effect is ignored. The

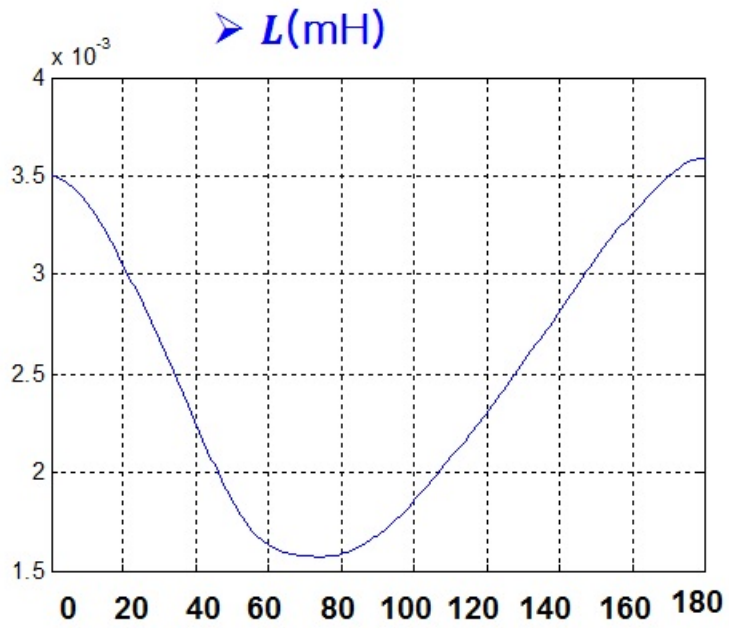


Figure 3.6: Inductance Profile for Pseudo-sinusoidal SRM

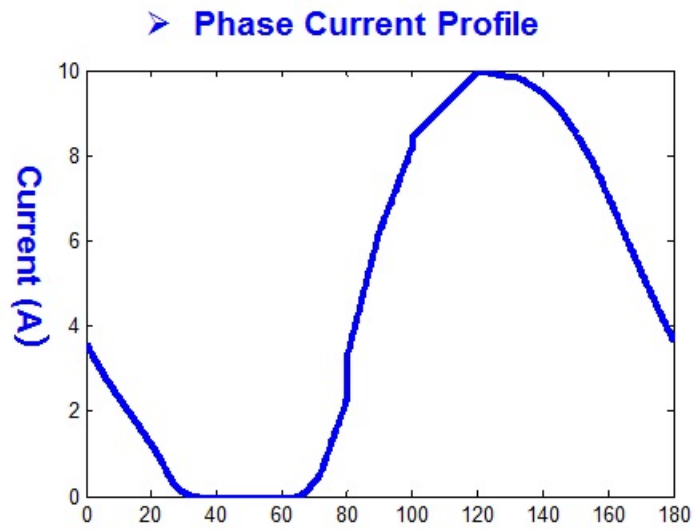


Figure 3.7: Current Profile for Pseudo-sinusoidal SRM

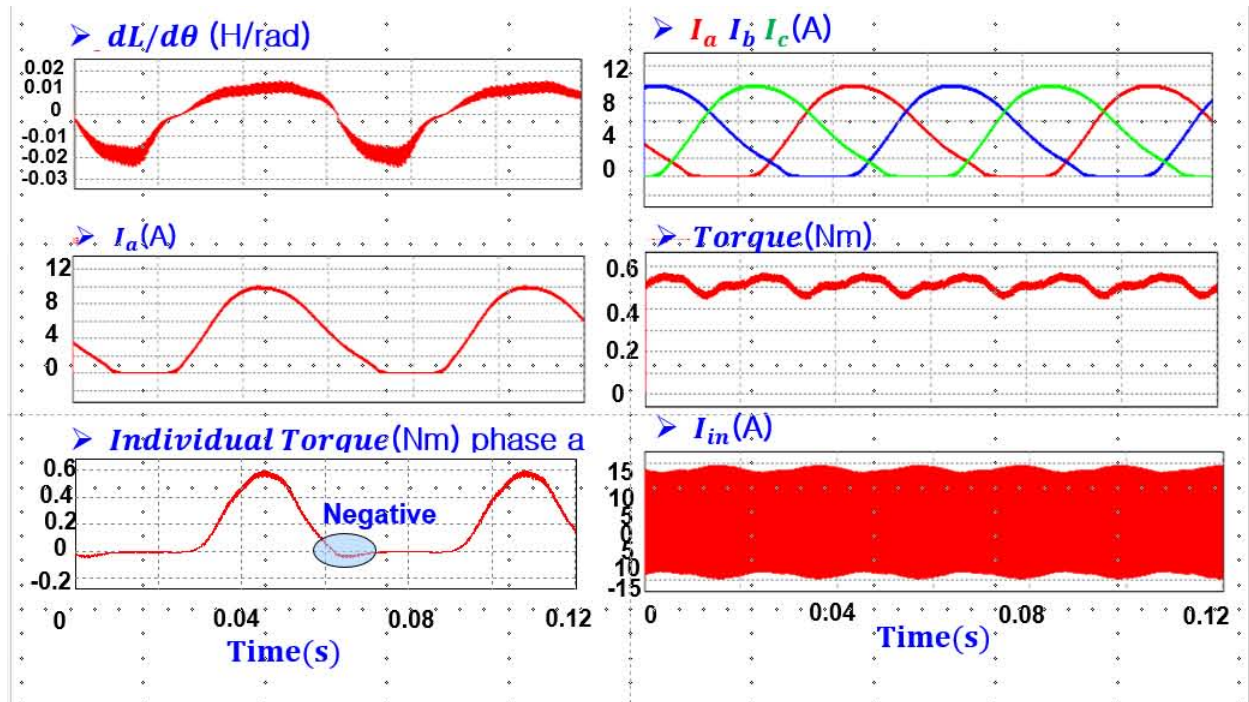


Figure 3.8: Simulation Result for Pseudo-sinusoidal SRM

current profile is made with slight tuning to reach a torque with less ripple. As is seen, the torque ripple is about 5 %. Ideally, the torque ripple can reach to zero if the current reference is calculated with no ripple tolerance, which would need much more computation time. The input bus current ripple during commutation interval for conventional method is greatly reduced in this case. The input current ripple is hardly seen by this new torque control method, therefore a small value high-reliability ceramic capacitor can be used across the input bus.

### 3.4 Summary

This chapter proposes a new torque control method for SRM. This control method is suitable for switched reluctance motor with ‘sinusoidal’ inductance profile. Simulation by MATLAB



Simulink and PSIM co-simulation is used to verify the effectiveness of this control method for both the idealized 'sinusoidal' SRM and the 'Pseudo-sinusoidal' SRM.

## Chapter 4

# Implementation of New Torque Ripple Minimization Algorithm

In order to verify the effectiveness of the new torque ripple control scheme, an experimental setup was built with the ‘Pseudo-Sinusoidal’ SRM designed by Dr. Ethan Swint. A digital current controller is designed to stabilize the system and track the current reference. A switched reluctance motor drive system consists of the following major parts: the motor, which is the executive component; the current controller, which controls the current profile; the position sensor; the power inverter which transfers the power from the power supply to the motor. This chapter gives the structure of the SRM drive system and will discuss each component of the SRM drive system separately in the following sections. The system software is also discussed briefly at the end of this chapter.

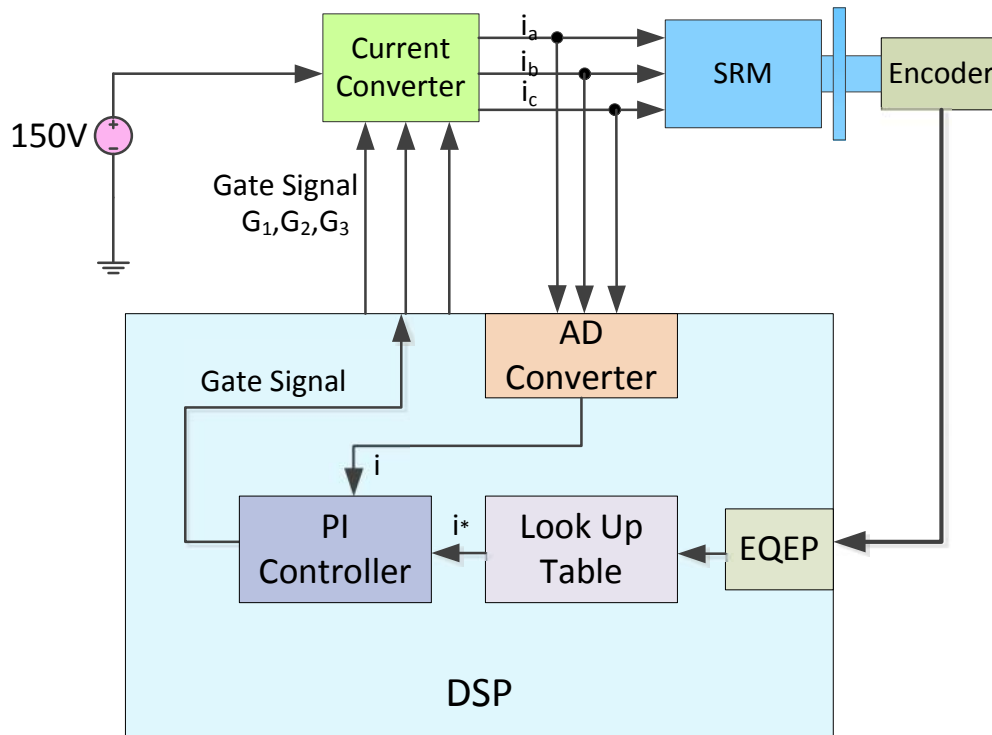


Figure 4.1: SRM Drive with Torque Control

## 4.1 Hardware Implementation

The SRM drive system with constant torque control consists of the following parts: the switched reluctance motor; current sensor which measured the SRM current value; the DSP controller, which accepts the SRM rotor position information, gives the reference current information and determine the power switches action with PI control; the position sensor which gives the rotor position; the power inverter which transfer and control the power from power supply to the SRM and the load motor. The structure of the SRM drive system is illustrated in Figure 4.1. Those SRM drive system components are discussed separately in the following sections.

### 4.1.1 Pseudo-Sinusoidal Switched Reluctance Motor

The motor used to implement the ripple free torque control algorithm is introduced in Ethan swint's dissertation, 2012. The inner structure of the motor is shown in Figure 1.1. From Figure 1.1, it can be seen that the switched reluctance motor has 12 stators and 16 rotors. The structure is very simple as there are only windings on the stators, no windings on the rotors. There is no magnetic materials used in the motor, hence the motor cost is much lower compared with other magnetic motors like permanent magnetic synchronous motor and the AC induction motor.

The key parameters for the switched reluctance motor is listed here.

Pase,number	3	Reference Speed	3520rpm
Reference Torque	0.81Nm	Reference Power	300W
Stator,max Width	123mm	Stator, max OD	132mm
Stator,min width	109mm	stack height	30mm
Airgap,min	0.25mm	Stator,min ID	69.0mm
Stator pole,arc	11.5°	Rotor, max OD	68.5mm
rotor pole,arc	6.5 °		

### 4.1.2 Power Stage

In this experiment, two three-phase power inverter are selected as the power stage to drive the motor. The 600V-20A 3phase IGBT inverter, Fairchild smart power module, FSBB20CH60C, is used as the main bridge of the full bridge inverter, which includes the control ICs for gate driving and protection. This inverter consists of 12 IGBTs. The input to the system is fixed at 150V DC and the maximum load current is to be designed at 10A,

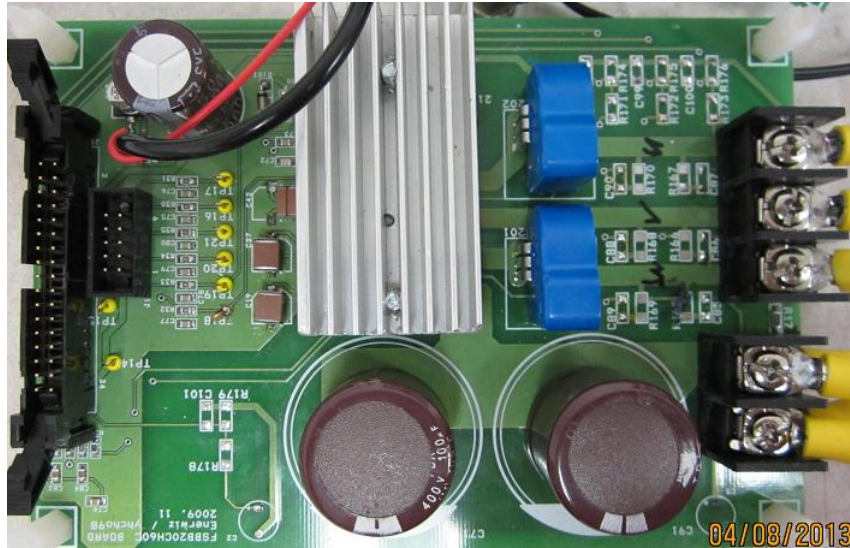


Figure 4.2: Power Stage

which are within the operating range of the smart power module. with which the current can flow in both direction. Three are six output terminals:  $A^+$ ,  $A^-$ ;  $B^+$ ,  $B^-$ ;  $C^+$ ,  $C^-$ . The PCB board of the power stage is shown in Figure 4.2

### 4.1.3 Current Sensor

The torque control is essentially a current control, hence, the current information needs to be firstly obtained by the current sensor before sent to the input of the Analog-to-Digital Converter for compensation. In this experiment, the reference current varies from 0 to 10A within one electrical angle cycle. Consider the case if the motor is running at high speed, the current sensing conversion should be fast enough without significant delay to guarantee that the current can follow the reference. Current Transducer LA150-P from LEM is selected the phase current transducer which is closed loop current transducer using the hall effect. A 165 $\Omega$  resistor is used to convert the current information to voltage information for the following stage of Analog to Digital Converter. The electrical data and the dynamic performance data



Figure 4.3: current transducer

are plotted in the following table.

primary continuous direct current(nominal)	150A
primary nominal current rms	106A
secondary current	75mA
secondary nominal current rms	53mA
conversion ratio	1:2000
supply voltage	( $\pm 5\%$ ) 15V

The primary nominal rms current is 150A, however, the maximum current for a individual phase is just 10A. Six turns of the phase wire are winded on the current transducer to make the equivalent maximum current equal to 60A, which is a proper value for the current transducer conversion range.

The conversion ratio of the current transducer is 1:2000, for 60A maximum current, the output current is 30mA. The input range of the second stage of the analog to digital converter is set to be  $\pm 10V$ , a  $165\Omega$  resistor convert the 30mA current to 4.85V voltage for analog-to-digital converter.

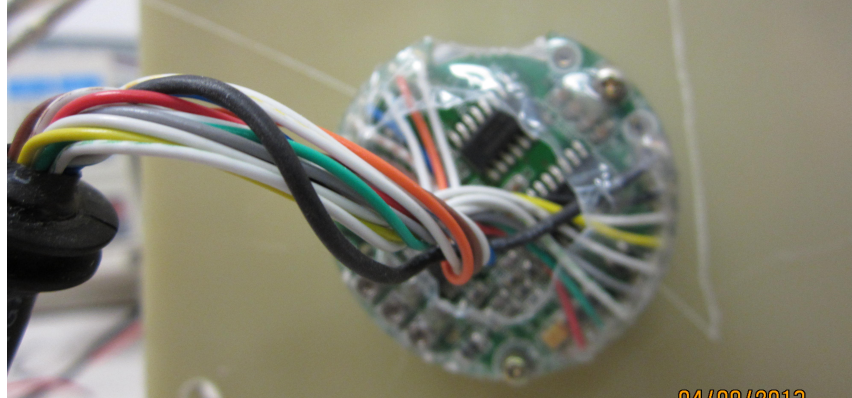


Figure 4.4: Encoder

#### 4.1.4 Position Acquisition

The switched reluctance motor is a highly nonlinear system. The system inductance is dependant on the rotor position  $\theta$ . The current reference also varies with the rotor position. The encoder needs to have enough accuracy to give the controller an accurate position information. LS H42 is selected to be encoder to sense the rotor position. The encoder generate 2000 pulses every revolution. The maximum speed for the encoder is 6000rpm. The encoder uses three output signals A,B and Z.

#### 4.1.5 DSP Board

Texas Instrument TMS320F28335 is selected as the micro-controller. TMS320F28335 is designed for motor control which has a lot features like, high-performance static CMOS technology; high-performance 32-bit CPU, and several high performance peripherals. TMS320F28335 has up to 150MHz system clock, 64 GPIOs, 18 PWM outputs, 8 32-bit CPU timers, 2 quadrature encoder interface. These integrated peripherals facilitates the control of the motor drive system. Its system structure is given by Figure 4.5

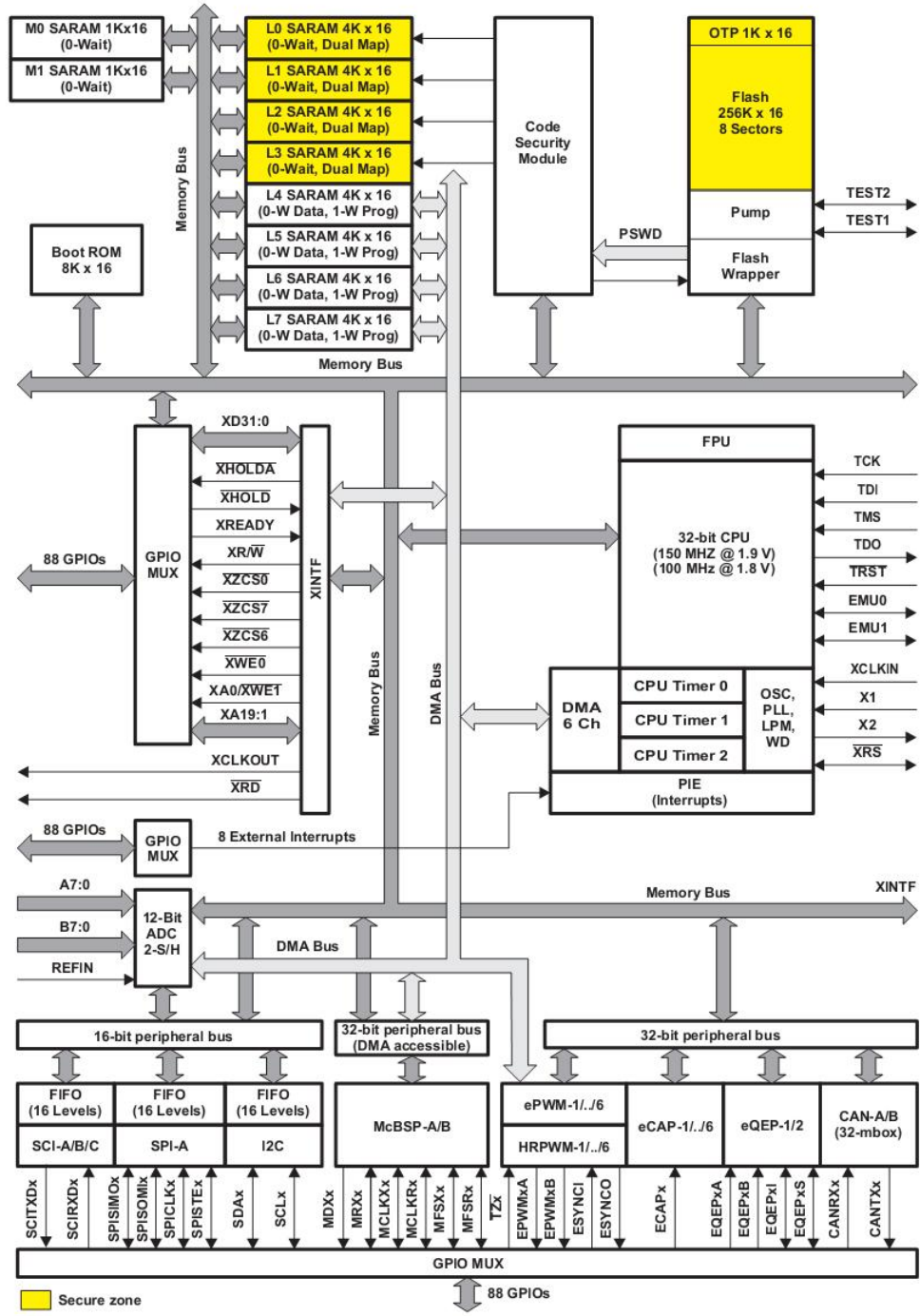


Figure 4.5: DSP Structure System



For DSP board, it functions as the major part of the control responsibility. The analog to digital converter receives the measured current information from the current transducer, converts the analog voltage information to digital current information. The EQEP module receives the rotor position information and put it to a look-up table stored in DSP to generate the reference current file. The digital PI current controller compares the difference between the real current and reference current and gives the duty cycle gate signals by ePWM module. The following session will discuss about each module seperately.

### **Analog to Digital Converter**

For torque control, the phase currents must be controlled to obtained the desired respective individual phase torques. Before controlling the currenst by the DSP controller and the inverter, the currents are sensed by current sensor and converted to digital quantities by the Analog to Digital Converter. For this experiment, an external AD converter AD7865 is selected due to its better feature (conversion time, accuracy) compared with DSP integrated ADC, the external AD embodies several high performance features as shown:

- (1) Fast conversion time ( $2.4\mu s$ ) with higher accuracy (14-bit ADC);
- (2) Wide selection of input ranges: AD7865 support  $\pm 10V, \pm 5V$  and  $\pm 2.5V$ ,  $0V$  to  $5V$  and  $0V$  to  $2.5V$

The converter also has other good features as it has four simutaneously sampled inputs, four  $0.35\mu s$  track/hold amplifiers, HW/SW select of channel sequence for conversion.

In this experiment, the Analog to Digital Converter is configured to accept  $\pm 10V$  input with MSB as the sign bit to show the polarity of the signal. The functional block diagram of AD7865 is shown in Figure 4.6

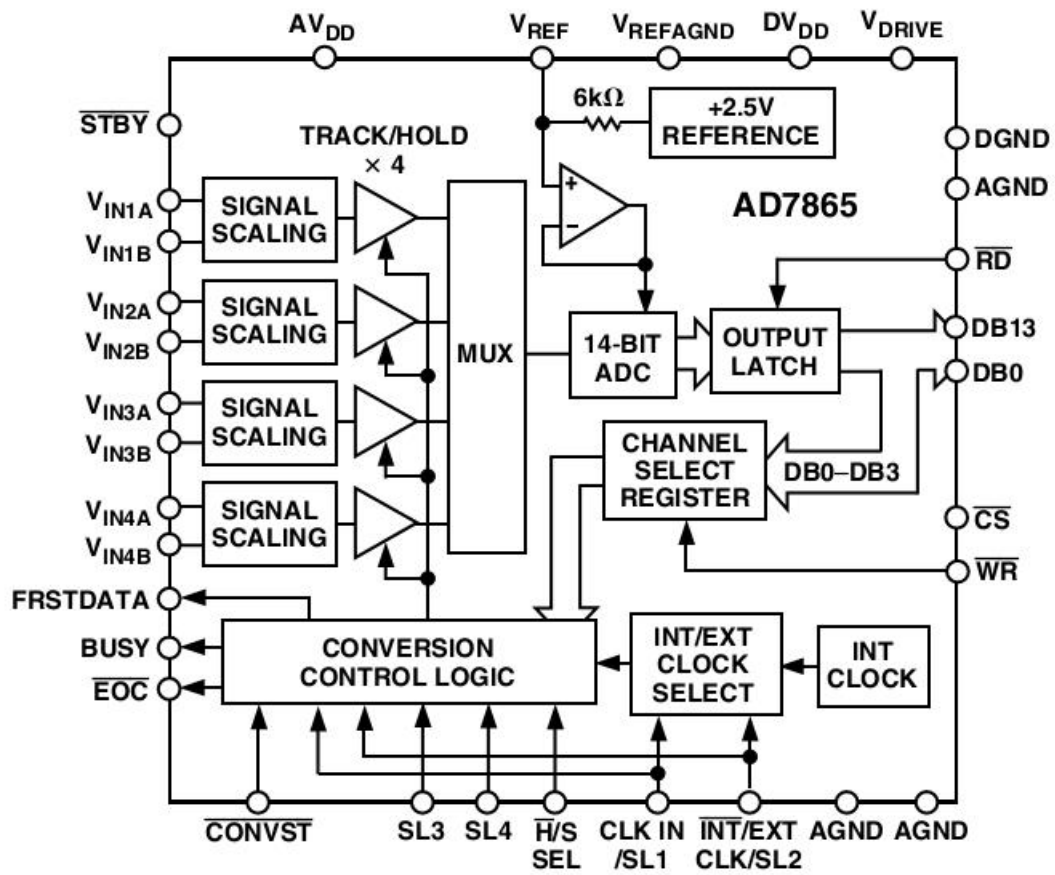


Figure 4.6: AD7865 Inner Structure

## Current Controller Design

Current is regulated by fixed-frequency PWM signals with varying duty cycles using PI control. The PI controller proportional gain  $K_p$  and integral gain  $K_i$  needs to be designed to get a fast and stable tracking to the current reference. A small signal model is derived by Xiaoyan Wang[57] in her thesis, with

$$G_{id} = \frac{2V_{dc}}{R_a + \omega K + sL} \quad (4.1)$$

However, the switched reluctance motor drive system is a nonlinear system, the inductance  $L$  and  $K$  varies with the rotor position, the output current duty-cycle transfer function contains a moving single pole. In order to design the current controller with this small signal model, worst case design should be considered. Even with this small signal model, the current controller is still difficult to be designed because the operating point for the switched reluctance drive would probably change. Trial and Error method is used to design the current controller. Finally, the current regulator is designed with proportional gain  $K_p = 5$  and integral gain  $K_i = 0.007$ , the PI controller function in DSP is

$$G_p(s) = K_p + \frac{K_i}{s} \quad (4.2)$$

With the PI controller, the compensation signal is generated. The compensation signals needs to go through the ePWM module to generate gate duty cycle signals. The ePWM module is configured to generate 10kHz PWM. At the beginning of each PWM signal period, an AD conversion interrupt service routine is called to gather the current information and rotor position and execute one PI compensation action. Finally, the compensation signal is going to compare with the PWM carrier to generate the PWM waveform. The DSP board

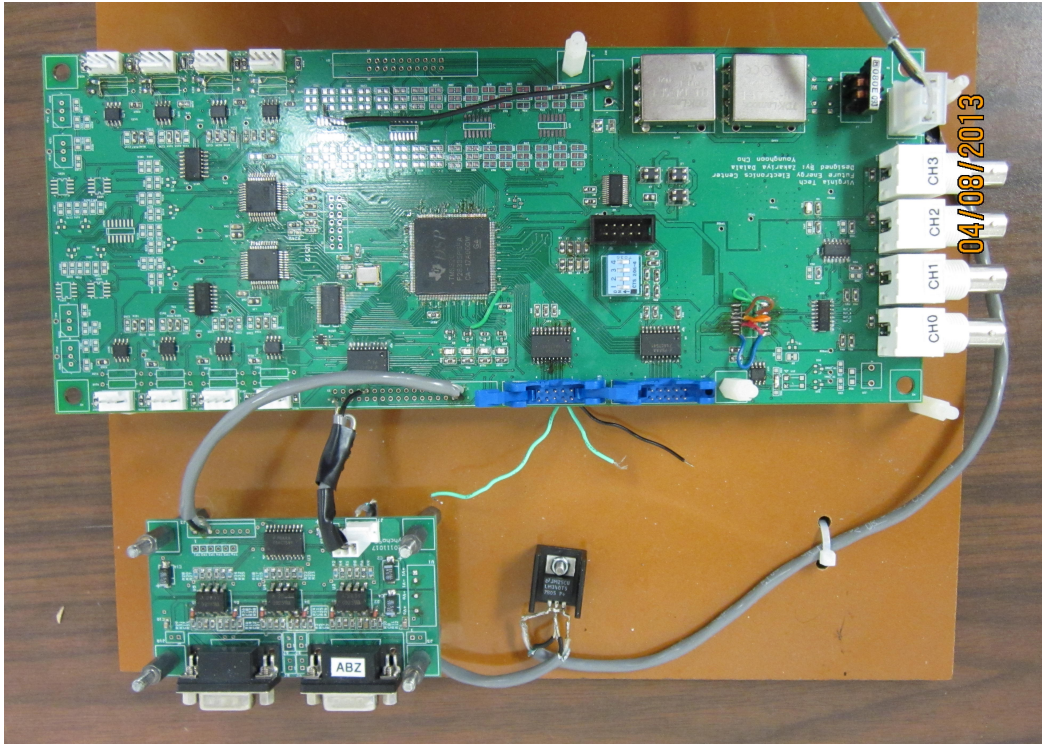


Figure 4.7: DSP Board

is shown in Figure 4.7

#### 4.1.6 Load Motor

The load motor is chosen with Marathon Electric AC induction motor. The motor reference speed is 3450rpm, with nominal 1/2 horse power. The motor is shown in Figure 4.8

Finally, the experimental setup is shown in Figure 4.9

## 4.2 Software Layout

The program was written with C language in Code Composer Studio shows the software structure for TMS320F28335 to control the switched reluctance motor. The whole software



Figure 4.8: Load Motor

consists of two part: the background dead-cycle program and an interrupt service routine. The program flow chart is given by Figure 4.10. At the highest level, the software consists of the initialization routines and run routines. The initialization routine contains the system clock configuration, the interrupt configuration, the initialization for each peripheral module. Upon completion of the necessary initialization, the background task is started. The background program is simply an infinite loop.

All of the motor control processing is done via interrupt service routines. This interrupt is called at the start of each period of the PWM carrier waveform. In the interrupt service routine, the DSP will acquire the rotor position and gives a current command at that rotor position, then acquire the current information from the AD converter, finally all the information is sent to the digital PI controller to give a compensation signal. The compensation signal compare with the PWM waveform and gives the duty cycle gating signals for the IGBT switches.

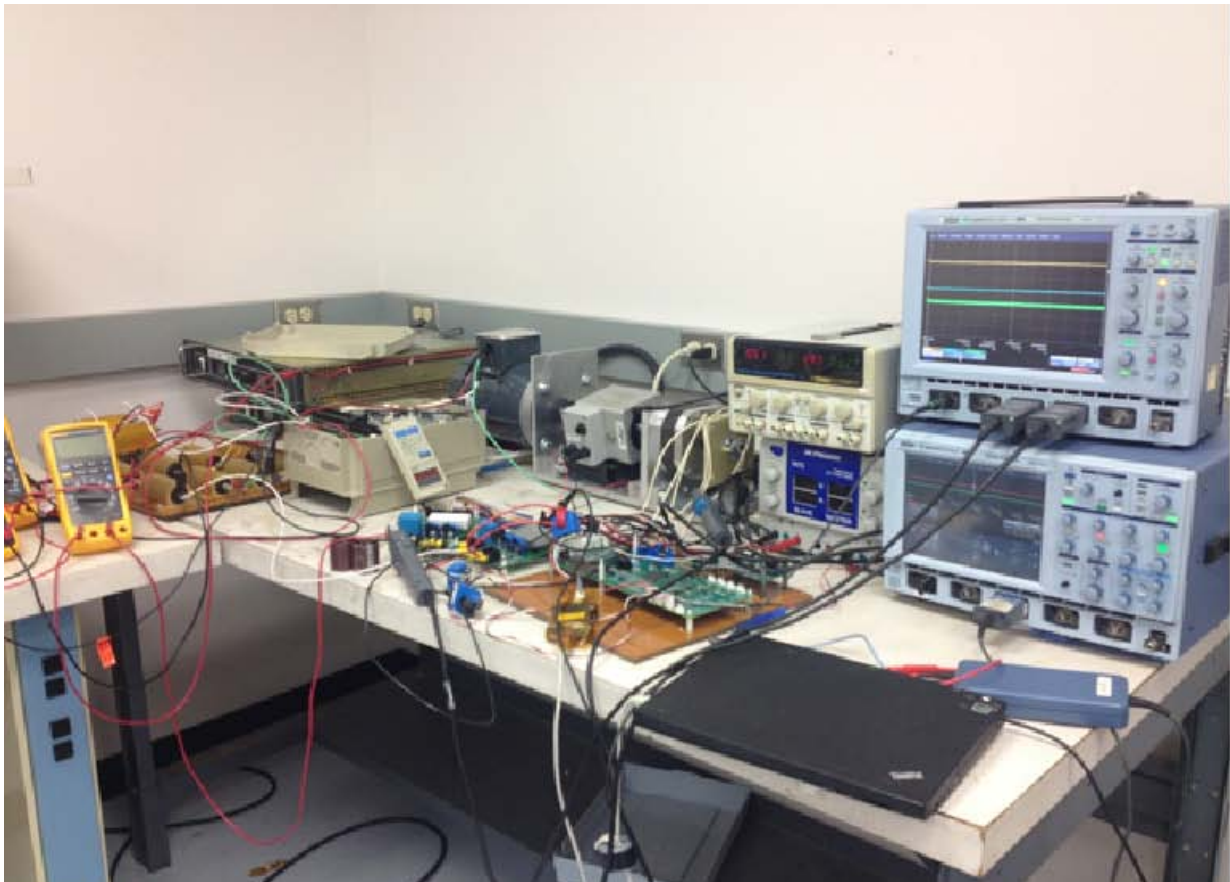


Figure 4.9: Experimental Setup

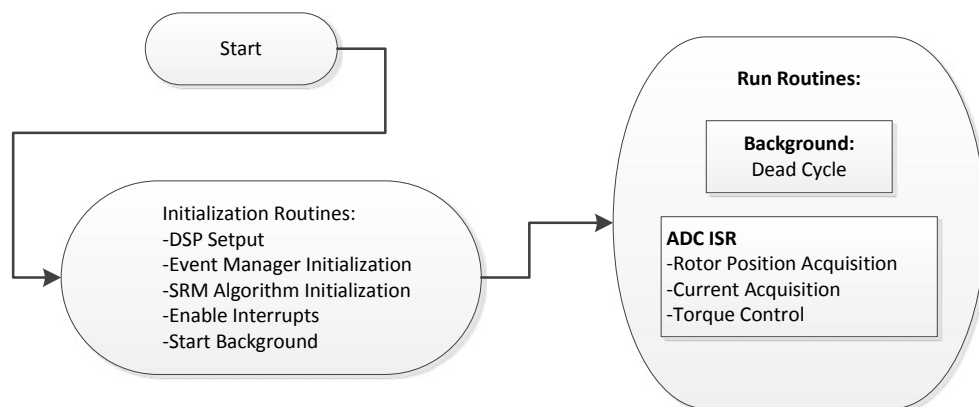


Figure 4.10: Program Flow Chart

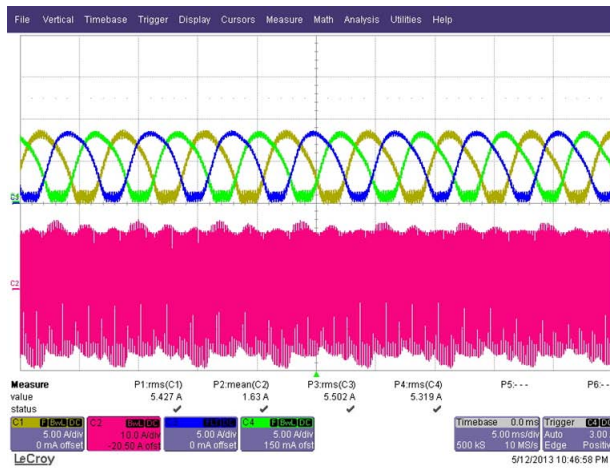
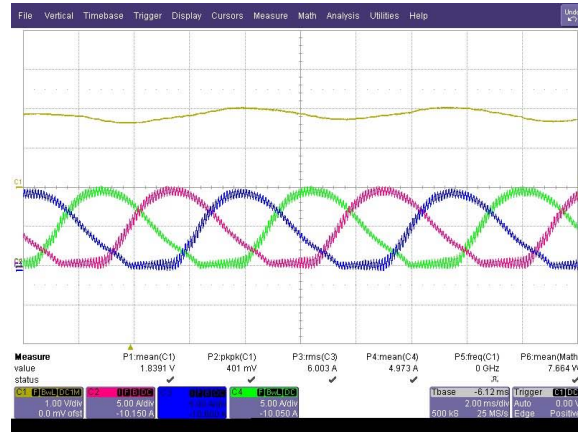


Figure 4.11: Experimental Result at 500rpm

### 4.3 Experimental Result

The motor used for experiments has same parameters with the simulation. The experimental results are shown in Figure 4.11 and 4.12.

In Figure 4.11, measurement unit of the oscilloscope is set to be 5A/div for phase current, 2.5lb/div for the torque. The torque was measured using the Himmelstein torque sensor, which has sufficient bandwidth to demonstrate the ripples at the experimental speeds. Figure 4.11 represents the motor running at 500rpm, while Figure 4.12 represents the motor running

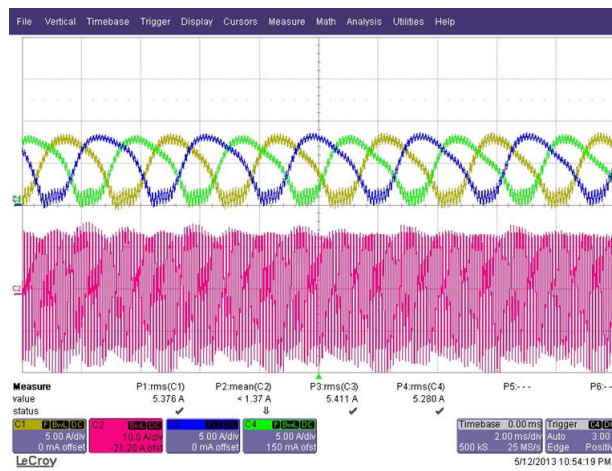
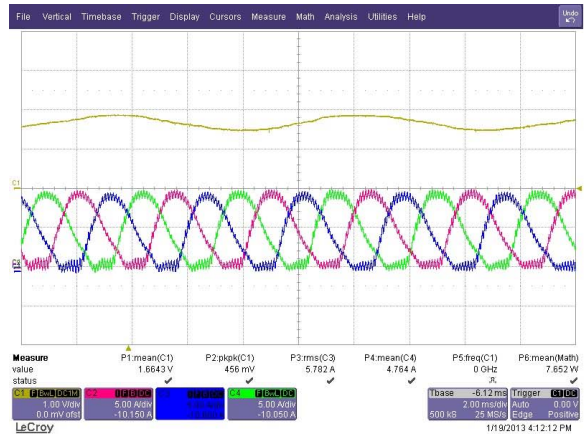



Figure 4.12: Experimental Result at 1000rpm



at 1000rpm. The torque is around 0.6Nm. From Figure 4.11 and Figure 4.12, the constant output torque object is reached, although there is still some low frequency noise ripple on it. However, it is not because of the SRM current control inaccuracy, since the noise frequency is not increased due to the increased motor speed as is shown in Figure 4.11. The input bus still has large current ripple with a constant average current. This is because of the nature of the chosen inverter topology. A new inverter topology to control the current should be invented to get a true smooth input bus current.

## 4.4 Summary

This section introduces the implementation of the proposed torque control method using ‘pseudo-sinusoidal’ current reference for switched reluctance motor drives. The hardware implementation for each functional block is explicit separately. The software layout is introduced in the latter part of this chapter. 

# Chapter 5

## Conclusions

### 5.1 Conclusion and Future Work

#### 5.1.1 Summary

Due to its doubly salient structure, the switched reluctance motor exhibits much more torque ripple compared with traditional AC and DC motors. The large torque ripple will result in speed variation, acoustic noise and mechanical vibration. Large electrolytic capacitors are also used to attenuate the current ripple at the input bus, which reduce the reliability of the SRM drive system. However, switched reluctance motor embodies several advantages that favored by the industry, such as simple structure, reduced cost, ruggedness, very high-speed operation capability. The switched reluctance has been used in several applications, though in some servo-type applications which require high control quality, the SRM application is slow due to its large torque ripple. Therefore, if the torque ripple can be reduced, the SRM can be a good substitute to the other AC or DC motors.

First, the origin of the torque ripple is presented. The existence of the inductance in the switched reluctance motor excludes the possibility that the current can track a rectangular reference. Therefore, the torque ripple and current ripple always happen at the commutation interval.

Next, considering the negative effect of the discontinuous current reference. A continuous current profile eliminating the torque ripple at commutation interval is proposed. Each time, the three phases are all conducted with current, eliminating the concept of conduction angle and commutation angle. Note that there are some negative torque produced at some intervals, the output torque is reduced because of the trade-off between the torque ripple and maximum torque per ampere.

Finally, the new current control scheme is verified by the simulation and the experimental result. Although there are some unknown low frequency noises, the output torque is near a constant which prove the effectiveness of the new current control scheme.

### **5.1.2 Future Works**

In the thesis, the new current control scheme bases on the assumption that the SRM is linearly magnetized, ignoring the saturation effect. It could be interesting to make further research on the new current control scheme considering the saturation effect to get a relatively high torque. Furthermore, the unknown low frequency noise needs to be studied to eliminate the disturbance to the actual result.

Besides, the inverter topology is another future work to realize constant input current. Currently, due to its modulation strategy, the input current ripple is still very large. Electrolytic capacitor is still needed, although the average current is a constant.

## 5.2 Publications

L. Du, B.Gu,J.Lai,“Control of Pseudo-Sinusoidal Switched Reluctance Motor with Zero Torque Ripple and Damped Input Current Ripple” , *ECCE,2013*

# Bibliography

- [1] T.J.E.Miller, "Switched reluctance motors and their control," Hillsboro, OH/Oxford, U.K. :Magna Physics /Oxford Science,1993.
- [2] I. Husain, "Minimization of torque ripple in SRM drives," *IEEE Trans. Ind. Electron.*, vol. 49, no.1,pp:28-39, Feb.2002.
- [3] X.D. Xue, K.W. E. Cheng, and S.L. Ho "Optimization and evaluation of torque-sharing functions for torque ripple minimization in switched reluctance motor drives," *IEEE Trans. Power Electron.*, vol.24, no.9, pp:2076-2090,Sept.2009.
- [4] M. Ilic-Spong, T.J.E. Miller, S.R. Macminn, and J.S. Thorp, "Instantaneous torque control of electric motor drives," *IEEE Trans. Power Electron*, vol. PE2, no.1,pp:55-61,Jan.1987.
- [5] D.S. Schramm, B.W. Williams, T.C. Green, "Torque ripple reduction of switched reluctance motors by phase current optimal profiling," *IEEE PESC'92*, vol.2, pp:857-860,1992.
- [6] Iqbal Husain and M. Ehsani, "Torque ripple minimization in switched reluctance motor drives by PWM current control," *IEEE Trans. Power Electron.*, vol.11, no.1,pp:83-88,

Jan.1996.

- [7] S. C. Shahoo, S.K. Panda, and J.X. Xu, "Determination of current waveforms for torque ripple minimization in switched reluctance motors using iterative learning: an investigation," *IEE Proc. Electric. Power Applicat.*, vol.146, no.4, pp:369-377, Jul. 1999.
- [8] S.K. Sahoo, S.K. Panda, and J.X. Xu, "Iterative learning-based high-performance current controller for switched reluctance motors," *IEEE Trans. Energy Convers.*, vol. 20, no.1, pp: 200-208, Jan. 2005.
- [9] S.K. Sahoo, S.K. Panda, and J.X. Xu, "Indirect torque control of switched reluctance motors using iterative learning control," *IEEE Trans. Power Electron.*, vol.20,no.1, pp:200-208, Jan.2005.
- [10] P.C. Kjaer, J.J. Gribble and T.J.E. Miller,"High-Grade control of switched reluctance machines",*IEEE Trans. Industry Applications*,vol.33, no.6, Nov./Dec. 1997.
- [11] C. Kim and I. Ha, "A new approach to feedback-linearizing control of variable reluctance motors for directive-drive applications," *IEEE Trans. Control Systems Technology*, vol.4,no.4,1996.
- [12] C. Choi, S. Kim, Y. Kim, and K. Park "A new torque control method of a switched reluctance motor using a torque-sharing function",*IEEE Trans. Magnetics*, vol.38, no.5, pp:3288-3290,Sept.2002.
- [13] D. Lee, S. Ahn, and J. Ahn "A simple negative torque compendation scheme for a high speed switched reluctance motor," *Journal of Power Electronics*, vol 12, no.1, pp:58-66,Jan. 2012.

- [14] D.G. Taylor M.Ilic-Spong, R. Marino, S. Peresada, “A feedback linearizing control for direct-drive robots with switched reluctance motors,” *Proc. 25th Conf. on Decision and Control*, vol.25 pp:388-396, Dec. 1986
- [15] M.Ilic-Spong,R.Marino, S.M.Peresada and D.G. Taylor, “Feedback linearizing control of switched reluctance motors,” *IEEE Trans. Automat. Contr.*, vol.32,no.5,pp:371-379, May 1987.
- [16] S.K. Panda,P.K. Dash, “Application of nonlinear control to switched reluctance motors: a feedback linearisation approach,”*IEE, Proc. Electron. Power Applicat.* vol.143,no.5,pp:371-379, Sept.,1996.
- [17] R.S. Wallace, D.G. Taylor, “A balanced commutator for switched reluctance motors to reduce torque ripple,” *IEEE Trans. Power Electronics* vol.7, no.4, pp:617-626,Oct.1992.
- [18] R.S. Wallace,D.G. Taylor,“Torque ripple reduction in three-phase switched reluctance motors,” *Conf. Amreican Contr.* pp: 1526-1527, May 1990
- [19] R.S. Wallace, D.G. Taylor,“Low-torque-ripple switched reluctance motors for direct-drive robotics,” *IEEE Trans. Robotics and automation.* vol.7, no.6,pp:733-742, Dec. 1991.
- [20] H.Bae and R. Krishnan, “A novel approach to control of switched reluctance motors considering mutual inductance,” *IEEE IECON 26th Annu. Conf.* vol. 1,pp:369-374,2000
- [21] V.I. Utkin, “Sliding modes applications in power electronics and motion control systems,” *Proc. IEEE Int. Sysosium on Ind. Electron.* vol.1,pp:TU22-TU31,1999.

- [22] V.I. Utkin, "Sliding modes in control and optimization," Springer-Verlag.1992.
- [23] T. Chuang and C. Pollock, "Robust speed control of a switched reluctance vector drive using variable structure approach," *IEEE Trans. Ind. Electron.* vol.44,no.6,pp:800-808,Dec.1997.
- [24] A. Forrai, "Sliding mode control of switched reluctance motor drive," *Procs. 6th Int. Con. OPTIM*, vol.2,pp467-472, May1998.
- [25] H. Yang, S.K. Panda, C.Y. Liang, "Performance comparison of sliding mode control with PI control for four-quadrant operation of switched reluctance motors", *Procs. 1996 Int. Conf. on Drives and Energy Systems for Industrial Growth*,vol.1, pp:381-387, 1996.
- [26] G.S. Buja,R.Menis, and M.I. Valla, "Variable structure control of an SRM drive," *IEEE Trans. Ind. Electron.* vol.40, No.1,pp:56-63,Feb.1993.
- [27] E. Bizkevelci, K. Leblebicioglu and H.B.Ertan, "A sliding mode controller to minimize SRM torque ripple and noise", *IEEE Int. Symposium on Ind. Electron.* vol.2,pp:1333-1338, May 2004
- [28] S.K.Sahoo,S.K.Panda,J.X.Xu "Direct torque controller for switched reluctance motor drive using sliding mode control," *IEEE PEDS,2005* vol.2. pp:1129-1134.2005.
- [29] A.M. Osama, H.A. Fattah, A.M. Sakr, "Variable structure flux linkage controller for torque ripple minimization in switched reluctance motors," *Procs. American Control Conf.* vol.4,pp:3105-3110,2002



- [30] W.Shang,S.Zhao,Y.Shen,Z.Qi,“A sliding mode flux-linkage controller with integral compensation for switched reluctance motor,”*IEEE Trans. Magnetics* vol:45,no.9,pp:3322-3328,2009
- [31] D.S.Reay, T.C.Green and B.W.Williams,“Application of associative memory neural networks to the control of a switched reluctance motor”,*Procs. IECON'93* vol.1,pp:200-206, 1993
- [32] D.S. Reay, T.C. Green, B.W. Williams,“Neural networks used for torque ripple minimisation from a switched reluctance motor,”*5th European conf. Power Electron. and Applicat.*vol.6, pp:1-6, Sept.1993.
- [33] J.G.O'Donovan,P.J.Roche, R.C. Kavanagh, M.G.Egan and J.M.D. Murphy,“Neural network based torque ripple minimisation in a switched reluctance motor,” *IECON '94*.vol.2,pp:1226-1231,Sept.1994.
- [34] C. Shang,D.Reay and B.Williams,“Learning rate functions in CMAC neural network based control for torque ripple reduction of switched reluctance motors”,*IEEE Int. Conf. on Neural Networks* vol.4,pp:2078-2083, Jun.1996.
- [35] Z. Lin,D.S.Reay,B.W.Williams,“Torque ripple reduction in switched reluctance motor drives using B-spline neural networks”,*4th IAS Annual Meeting* vol.4,pp:2726-2733,2005
- [36] K.M.Rahman,A.V.Rajarthnam,M.Ehsani,“Optimized instantaneous torque control of switched reluctance motor by neural network,”*IEEE IAS Annu. Meeting '97*, vol.1,pp:556-563.1997.

- [37] B.Fahimi,G.Suresh,K.M.Rahman,M.Ehsani,“Mitigation of acoustic noise and vibration in switched reluctance motor using neural network based current profiling”,*3rd IAS* vol.1,pp:715-722,1998
- [38] K.M.Rahman,S.Gopalakrishnan,B.Fahimi,A.V.Rajarithnam,“Optimized torque control of switched reluctance motor at all operational regimes using neural network,” *IEEE Trans. Ind. Applicat.*vol.37,pp:701-708,May/June 2001
- [39] S. Bolognani, “Fuzzy logic control of a switched reluctance motor drive,” *IEEE Trans. Ind. Applicat.*vol.32,no.5,pp:1063-1068,Sept/Oct. 1996
- [40] M.G.Rodrigues,W.I.Suemitsu,P.Branco,J.A.Dente,L.G.B.Rolim,“Fuzzy logic control of a switched reluctance motor”,*Procs. ISIC* vol.2,pp:527-531,1997
- [41] S.Mir, M.E.Elbuluk, I.Husain, ”Torque-ripple minimization in switched reluctance motors using adaptive fuzzy control,” *IEEE Trans. Ind. Applicat.* vol.35,no.2,pp:461-468,March/April,1999
- [42] M.J. Kharaajoo,H.Ebrahimirad ”Fuzzy logic torque ripple minimization of switched reluctance motors,” *Int. Symposium SCS* vol.1,pp:105-108,2003
- [43] A.Derdiyok, N.Inanc, V.Ozbulur, M.O.Bilgic, ”Improving performance of switched reluctance motor by fuzzy logic controller,” *Int.J.Robust Nonlinear control* vol.9,pp:307-317,1999
- [44] L.Huang, H.Sun, G.Song, J.Chu, ”A fuzzy-logic-based torque ripple reduction method for switched reluctance motors,” *Proc. 2nd Int. conf. machine learning and cybernetics* vol.5,pp:2-5,Nov.2003.

- [45] L.O.A.P.Henriques, L.G.B. Rolim, W.I.Suemitsu, P.J.C.Branco, J.A.Dente, "Torque ripple minimization in a switched reluctance drive by neuro-fuzzy compensation," *IEEE Trans. Magnetics* vol.36,no.5,pp:3592-3594,2000
- [46] L.Kalaivani,N.S.Marimuthu,P.Subburaj, "Intelligent control for torque-ripple minimization in switched reluctance motor," *21st ICCES* pp:182-186,Jan.2011
- [47] N.C.Sahoo,S.K.panda, "Low torque ripple control of switched reluctance motors using iterative learning," *IEEE Trans. Energy Conversion* vol.16,No.4,pp:318-326,Dec.2001
- [48] S.K.Sahoo,S.K.Panda,J.X.Xu "Iterative learning-based high-performance current controller for switched reluctance motors," *IEEE Trans. Energy Conversion*,vol.19,no.3,pp:491-498,Sept. 2004
- [49] S.K.Sahoo,S.K.Panda,J.Xu "Indirect torque control of switched reluctance motors using iterative learning control," *IEEE Trans. Power Electronics*,vol.20,no.1,pp:200-208,Jan,2005
- [50] S.K.Sahoo,S.K.Panda and J.X.Xu, "Iterative learning control based direct instantaneous torque control of switched reluctance motors," *35th PESC '04* vol.6,pp:4832-4837,2004.
- [51] R.Krishnan, "Switched reluctance motor drives," Taylor&Francis,2001
- [52] G.Dunlop, "A switched-reluctance motor drive with zero torque ripple and a constant inverter bus current," ARCHIVE:*Proc. Institution of Mechanical Engineers,Part I: Journal of Systems and Control Engineering 1991-1996 (vols 205-210)*,vol.208,no.19,pp:61-68,Jun.1994.

- [53] E.B.Swint, "DC reluctance machine-a doubly-salient reluctance machine with controlled electrical and mechanical power ripple," Ph.D. Dissertation, Virginia Tech, 2012.
- [54] E.B.Swint, "Switched reluctance motor without torque ripple or electrolytic capacitors," *IEEE ECCE '2011*, pp:1657-1663, Sept. 2011
- [55] X. Wang, "Modeling and Implementation of Controller for Switched Reluctance Motor With Ac Small Signal Model," M.S. Thesis, Virginia Tech, 2001